

A

Dissertation on

*Adsorptive removal of Rhodamine B (dye) using low cost adsorbents*

Submitted in Partial Fulfillment for the Award of the Degree

of

Master of Technology (Chemical Engineering)

**Akash Kumar**

Roll No. 211CH1259

*Under the supervision of*

**Dr. Arvind Kumar**



Department of Chemical Engineering

**National Institute of Technology, Rourkela**

**2012-13**



Department of Chemical Engineering

**National Institute of Technology, Rourkela**

---

### **CANDIDATE'S DECLARATION**

I hereby declare that the work, which is being presented in the dissertation entitled **“Adsorptive Removal of Rhodamine B (Dye) using low cost Adsorbents”** in the partial fulfillment of the requirements of the award of the degree of Master of Technology in Chemical Engineering, submitted in the Department of Chemical Engineering, National Institute of Technology, Rourkela, Odisha, is an authentic record of my own work carried out during the period of July 2012 to May 2013 under the supervision of **Dr. A. Kumar**, Assistant Professor, Department of Chemical Engineering, National Institute of Technology, Rourkela, Odisha.

I have not submitted the matter, embodied in this dissertation for the award of any other degree.

**Date:**

**Akash Kumar**

**Place: Rourkela**

This is to certify that the above statement made by the candidate is correct to the best of my knowledge.

**Date:**

**(Dr. Arvind Kumar)**

Supervisor

## ACKNOWLEDGEMENT

I would like to make my deepest appreciation and gratitude to Dr. Arvind Kumar, my project supervisor for this project work, for his valuable guidance, constructive criticism and encouragement during every stage of this project work.

I am thankful to Prof. R. K. Singh, HOD, Chemical Engineering Department, NIT, Rourkela for being uniformly excellent advisor. He was always open, helpful and provided strong broad idea.

I owe a depth of gratitude to all department faculties of Chemical Engineering Department, NIT, Rourkela for their small but important advice related to project work. I would like to give special thanks to all staffs of the Chemical Engineering department for their all-time technical, moral support to carrying out the project.

Thanks to my M. Tech classmates Mr. Sowhm Swain Mohapatra, Mr. Shrirang Sabde and Mr. Lalan Singh Yadav, PhD scholar for helped me a lot in carrying out the experiments and for proper discussion about tit bit of this project work. Also thanks to all inmates in Rourkela, for whom life in Rourkela was most memorable in my whole life.

Department Metallurgical & Materials Engineering and Chemistry Department supported a lot for carrying out different characterization tests and analysis, which were crucial part for my project.

Finally, I thank to God and to my loveable parents, grandparents and dear sister without them this would not possible. Their faith, support and love for me are unbelievable, which gave me a unpredictable strength and patience in my life.

**AKASH KUMAR**

**ROLL NO: 211CH1259**

## ABSTRACT

There is a regular industrial practice of disposing or emitting of chemical dye material to environment in the form of liquid effluent, which is a matter of global concern. Dyes are widely used in several industries like textile, dyeing, paper and pulp, tannery, paint industries etc. Dyes are considered an objectionable type of pollutant because they are toxic in nature and can be detected from bare eyes. Their classification can be done based on their usage, group and solubility. Various treatment processes used for the removal of dyes include adsorption, microbial degradation, wet air oxidation, ion exchange etc. Low cost adsorbents are available option for dyes removal from aqueous effluents. However, high cost of commercial adsorbents like activated carbon and others, material are losses during their usage, but by regeneration pose can be a best utilization of costlier adsorbent.

Four different adsorbents were self-prepared in laboratory from *Aegle marmelos* Shell, *abrus precatorius* seed, *azadirachta indica* (neem) seed and Mahua seed, which are all raw biomass. The adsorbents were characterized for BET surface area, point of zero charge, CHNS, TGA, SEM, FTIR etc.

Rhodamine B (RhB) basic dye, removal from the wastewater using adsorbents, activated mahua seed carbon (AMC) and activated neem seed carbon (ANC) among four self-prepared adsorbents.

Here batch studies were conducted to evaluate the effect of adsorbent dose, contact time, pH, initial concentration at 25 °C. The equilibrium adsorption data of RhB (dye) on adsorbent were analysed by the Langmuir, Freundlich and Temkin isotherm models. The isotherm data were well described by the Freundlich isotherm model. Pseudo-first-order, pseudo-second-order models were used to analyze the kinetic data obtained at different concentrations. The adsorption kinetics was well described by the pseudo-second-order kinetic model. For RhB-AMC and RhB-ANC system maximum adsorption capacity were found to 39.683 mg/g and 15.152 mg/g respectively at 65 °C. Adsorption experiment has carried out to show that maximum adsorption and it observed in acidic medium for AMC and basic medium for ANC.

**Key words:** Rhodamine B (RhB), Point Zero Charge ( $\text{pH}_{\text{pzc}}$ ), Activated Mahua Carbon (AMC), Activated Neem Carbon (ANC), Adsorption Isotherms, Equilibrium, Kinetics.

# CONTENTS

CERTIFICATE	ii
ACKNOWLEDGEMENT	iii
ABSTRACT	iv
 1. INTRODUCTION	 1
2. LITERATURE REVIEW	5
2.1 Principle of adsorption	5
2.1.1 <i>Adsorption</i>	5
2.1.2 <i>Adsorbate</i>	5
2.1.3 <i>Adsorbent</i>	5
2.1.4 <i>Energy of adsorption</i>	6
2.1.5 <i>Types of adsorption</i>	6
2.1.5.1 <i>Physical adsorption</i>	6
2.1.5.2 <i>Chemical adsorption</i>	7
2.1.6 <i>Nature of adsorption</i>	7
2.2 Review on Rhodamine B dye removal	8
 3. MATERIAL AND METHOD	 15
3.1 Materials	15
3.2 Instruments	15
3.3 Adsorption Depends Upon Several Factors	16
3.4 Adsorbent Properties	16
3.4.1 <i>Physico-chemical properties of sorption</i>	16
3.4.2 <i>pH</i>	17
3.4.3 <i>Boehm Titration</i>	18
3.5 Raw material for adsorbent preparation	18
3.5.1 <i>Steps of adsorbent preparation</i>	22
3.6 Adsorbate	23
3.6.1 <i>Rhodamine B dye</i>	23
3.6.1.1 <i>Physical properties of adsorbate</i>	24
3.7 Principle of colour chemistry	24
3.8 Preparation of standard stock Rhodamine B solution	25
3.8.1 <i>Analytical measurement of Rhodamine B dye</i>	25
3.9 Adsorption Studies	25
3.9.1 <i>Experimental methodology used for the adsorption</i>	26
3.10 Batch contact system adsorption studies	26
3.11 Optimization of operational Variable	27
3.11.1 <i>Effect of adsorbent dose</i>	27
3.11.2 <i>Effect of contact time</i>	27
3.11.3 <i>Effect of pH</i>	27
3.11.4 <i>Effect of initial concentration</i>	27
3.11.5 <i>Effect of temperature</i>	28
3.12 Thermodynamic studies	28
3.13 Modeling of adsorption isotherms and its studies	29
3.13.1 <i>Langmuir isotherm</i>	29

3.13.2	Freundlich isotherm	30
3.13.3	Temkin isotherm	31
3.13.4	D-R isotherms	31
3.14	Adsorption Dynamics	32
3.14.1	Pseudo first order model	32
3.14.2	Pseudo second order model	33
4.	RESULT AND DISCUSSION	34
4.1	Calibration curve	34
4.2	Various operational parameters effect on adsorption of RhB-AMC system	35
4.2.1	<i>Effect of adsorbent (AMC) Dosage on adsorption</i>	35
4.2.2	<i>Effect of Contact Time</i>	36
4.2.3	<i>Effect of pH on RhB-AMC system</i>	37
4.2.4	<i>Point zero charge for RhB-AMC system</i>	38
4.2.5	<i>Effect of initial Concentration of RhB-AMC system</i>	39
4.2.6	<i>Kinetic Of Adsorption</i>	41
4.2.6.1	<i>Pseudo 1<sup>st</sup> order kinetic model</i>	41
4.2.6.2	<i>Pseudo 2<sup>nd</sup> order kinetic model</i>	42
4.2.7	<i>Effect of Temperature for RhB-AMC system</i>	42
4.2.8	<i>Adsorption equilibrium study</i>	43
4.3	Various operational parameters effect on adsorption of RhB-ANC system	46
4.3.1	<i>Effect of adsorbent dosage on RhB-ANC system</i>	46
4.3.2	<i>Effect of Contact time</i>	47
4.3.3	<i>Effect of pH</i>	47
4.3.4	<i>Effect of point zero charge</i>	48
4.3.5	<i>Effect of initial concentration</i>	49
4.3.6	<i>Adsorption Kinetics for RhB-ANC system</i>	50
4.3.6.1	<i>Pseudo 1<sup>st</sup> order Kinetic model</i>	50
4.3.6.2	<i>Pseudo 2<sup>nd</sup> order Kinetic model</i>	51
4.3.7	<i>Effect of Temperature</i>	51
4.3.10	<i>Adsorption equilibrium study for RhB - ANC system</i>	52
5.	CHARACTERIZATION OF ADSORBENTS	55
5.1	Thermo Gravimetry analysis (TGA)	56
5.2	Fundamental of TGA	55
5.2.1	<i>TGA of Mahua seed</i>	56
5.2.2	<i>TGA of Aegle Marmelos (Bael) Shell</i>	56
5.2.3	<i>TGA of Neem Seed</i>	57
5.2.4	<i>TGA of Abrus Precatorius Seed</i>	57
5.3	Proximate Analysis	58
5.4	SEM (Scanning Electron Microscope)	60
5.5	BET Analysis	62
5.6	Fourier Transform Infra-Red spectroscopy (FTIR)	63
	CONCLUSION	66
	FUTURE WORK	67
	REFERENCE	68

## LIST OF FIGURES

<i>Figure No.</i>	<i>Name of the Figure</i>	<i>Page No.</i>
Figure 2.1	Schematic representation of adsorption mechanism	05
Figure 3.1	Systematic preparation of Seed to Activated Carbon from <i>Madhuca longfolia</i> (Mahua)Seed	19
Figure 3.2	Systematic pictorial preparation of Bael Shell to Activated Bael Carbon	20
Figure 3.3	Systematic preparation of raw seed to Activated Azadirachta indica Carbon (Neem Seed)	21
Figure 3.4	Systematic preparation of raw Seed to Activated Abrus Precatorius seed Carbon (Crab's Eye)	22
Figure 4.1	Graphical representation of calibrating of unknown RHB dye concentration in the water sample, $C_0 = 0$ mg/l to 20 mg/l	34
Figure 4.2	Graphical presentation of adsorbent dosage effect on adsorption process, $V=50$ ml, $C_0=100$ mg/g, adsorbent dosage =0.2g to 2.2g, Stirring period =360 minutes, Natural pH & at aerobic condition	36
Figure 4.3	Graphical representation of contact time effect on adsorption process, $V=50$ ml, $C_0 = 100$ mg/g, Adsorbent dose = 0.5g/50 ml dye solution, Stirring period =15 to 360 minutes (with interval of 15 or 60 min),at natural pH	37
Figure 4.4	Graph of pH effect on adsorption process, $V=50$ ml, $C_0=100$ mg/g, Adsorbent dosage =0.5 g/50 ml of dye solution, Stirring period =180 minutes, pH = 2 to 12 (maintained)	38
Figure 4.5	Graph of $pH_{zpc}$ effect on adsorption process, $V=50$ ml, $C_0=100$ mg/g, Adsorbent Dosage = 1 g/50 ml of dye solution, Stirring time =180 minutes, pH = 2 to 13 (maintained)	38
Figure 4.6	Graphical representation of initial pH vs (initial pH– final pH)	39
Figure 4.7	Graphical representation of initial concentration effect on adsorption process, $V=50$ ml, $C_0=100$ mg/g, Dosage = 0.5 g/50 ml of dye solution, Stirring time =180 minutes, pH = 4.0 (maintained)	40
Figure 4.8	Pseudo first order kinetic model for AMC –RhB system; Adsorbent Dosage =0.5g/50 ml of dye solution, $C_0= 50,100$ and 150 mg/g,pH = 4.0 (maintained)	41
Figure 4.9	Pseudo second order kinetic model for AMC –RhB system; Adsorbent Dosage =0.5g/50 ml of dye solution, $C_0= 50,100$ and 150 mg/g	42
Figure 4.10	Effect of Temperature on adsorption process, $V=50$ ml, $C_0=100$ mg/g, Dosage = 0.5 g/50 ml of dye solution, Stirring time =180 min, pH=4	42

Figure 4.11	Langmuir isotherm for RhB- AMC system	43
Figure 4.12	Freundlich isotherm for RhB- AMC system	44
Figure 4.13	Temkin isotherm for RhB- AMC system	44
Figure 4.14	D-R isotherm for RhB – AMC system	45
Figure 4.15	Graphical presentation of adsorbent dosage effect on adsorption process, V=50 ml, C <sub>0</sub> =100 mg/g, adsorbent dose =0.2g to 3.0g, Stirring period =360 minutes, Natural pH, T = 25 °C for RhB-ANC system	46
Figure 4.16	Time effect on adsorption process, V=50 ml, C <sub>0</sub> =100 mg/g, Dose =1.2g/ 50 ml of dye solution, Stirring period =360 minutes, Natural pH, T = 25 °C	47
Figure 4.17	Graph of pH effect on adsorption process, V=50 ml, C <sub>0</sub> =100 mg/g, Adsorbent dosage =1.2 g/50 ml of dye solution, Stirring period =240 minutes, pH = 2 to 12, T = 25 °C	48
Figure 4.18	Graph of point zero charge, pH <sub>PZC</sub> , V=50 ml, C <sub>0</sub> =100 mg/g, Dose = 1g/50 ml of dye solution, Stirring time = 240 minutes, pH = 2 to 12, T = 25 °C	48
Figure 4.19	Graphical representation of initial concentration effect on adsorption process, V=50 ml, C <sub>0</sub> =100 mg/g, Dosage = 1.2 g/50 ml of dye solution, Stirring time =240 minutes, pH = 12.0 (maintained), T = 25 °C	49
Figure 4.20	Pseudo first order kinetic model for AMC –RhB system; adsorbent Dose = 1.2g/50 ml of dye solution, C <sub>0</sub> = 50,100 and 150 mg/g, pH = 12	50
Figure 4.21	Pseudo second order kinetic model for RhB-ANC system	51
Figure 4.22	Adsorption equilibrium of different temperature for RhB –ANC system	51
Figure 4.23	Langmuir isotherms for RhB-ANC system	52
Figure 4.24	Freundlich isotherm for RhB-ANC system	53
Figure 4.25	Temkin isotherm for RhB-ANC system	53
Figure 4.26	D-R isotherm studies for RhB- ANC system	54
Figure 5.1	TGA of raw Madhuca longfolia (Mahua) seed	56
Figure 5.2	TGA of raw Aegle Mermelos (bael) shell	56
Figure 5.3	TGA of raw Azadirachta indica (Neem) Seed	57
Figure 5.4	TGA of raw Abrus Precatorius (Crab's eye) seed	57
Figure 5.5	FTIR spectra of virgin and dye loaded Activated Mahua seed Carbon	64
Figure 5.6	FTIR spectra of virgin and dye loaded Activated Neem seed Carbon	65



## **LIST OF TABLES**

<b>Table No.</b>	<b>Table Title</b>	<b>Page No.</b>
Table 3.1	Details of instruments used during the research work	15
Table 3.2	Physicochemical properties of adsorbent	17
Table 3.3	pH measurement Results	18
Table 3.4	Scientific Classification of <i>Madhuca longfolia</i> (Mahua)seed	19
Table 3.5	Scientific Classification of <i>Aegle Marmelos</i> (Bael) Shell	20
Table 3.6	Scientific Classification of <i>Azadirachta indica</i> (Neem) seed	21
Table 3.7	Scientific Classification of <i>Abrus Precatorius</i> (Crab's Eye) seed	22
Table 3.8	Physical Properties of adsorbate	24
Table 4.1	Pseudo-first-order kinetic constants for the RhB- AMC adsorption system	41
Table 4.2	Pseudo-second-order kinetic constants for the RhB- AMC adsorption system	42
Table 4.3	Langmuir isotherm parameters for RhB- AMC adsorption system	43
Table 4.4	Freundlich isotherm parameters for RhB- AMC adsorption system	44
Table 4.5	Temkin isotherm parameters for RhB- AMC adsorption system	44
Table 4.6	D-R isotherms Parameters for RhB- AMC adsorption system	45
Table 4.7	Pseudo-first-order kinetic constants for the RhB- ANC adsorption system	50
Table 4.8	Pseudo-second-order kinetic constants for the RhB- ANC adsorption system	51
Table 4.9	Langmuir isotherm parameters for RhB- ANC adsorption system	52
Table 4.10	Freundlich isotherm parameters for RhB- ANC adsorption system	53
Table 4.11	Temkin isotherm parameters for RhB- ANC adsorption system	54
Table 4.12	D-R isotherms Parameters for RhB- ANC adsorption system	54
Table 5.1	Proximate Analysis data (%) (Dry basis)	59
Table 5.2	Ultimate Analysis data (%) (Dry basis)	60
Table 5.3	BET analysis data	62

## Nomenclature

$C_0$	: Initial concentration of Rhodamine B dye
$C_t$	: Final concentration of Rhodamine B dye
m or M	: Mass of adsorbent in grams
V	: Volume of the Rhodamine B solution
$Q_e, q_e$	: Amount of Rhodamine B adsorbed per unit mass of the adsorbent
$Q, q$	: The amount of Rhodamine B is adsorbed at time t (min)
% R	: Removal of Rhodamine B in percentage
$Q_0$	: Maximum adsorption capacity (Langmuir parameter)
$K_1$	: Rate constant of pseudo-first-order kinetics
$K_2$	: Rate constant of pseudo-second-order kinetics
$K_L$	: Free energy of adsorption (Langmuir parameter)
$Q_{max}$	: Monolayer adsorption capacity,mg/g
$b_L$	: Langmuir isotherm Constant
$K_T$	: the equilibrium binding constant (L/mg)
$K_F$	: Freundlich adsorption coefficient
$B_1$	: Related to the heat of sorption.
$\emptyset_D$	: Adjustment parameter in D-R equation ,mg/g
$\Psi_D$	: Adjustment parameter in the DR isotherm
$\beta$	: Constant of the D-R isotherm
$\Delta H^0$	: Change of Enthalpy of adsorption at standard state, J/mol
$\Delta G^0$	: Change in Gibb's free energy of adsorption at standard state, J/mol
$\Delta S^0$	: Change in the entropy for adsorption at standard state, J/mol
TGA	: Thermo Gravimetry Analysis
SEM	: Scanning electron microscope
BET	: Brunauer-Emmett-Teller (Surface area Analysis)
FTIR	: Fourier transform infrared spectroscopy
CHNS	: Ultimate analysis
RPM	: Revolutions per minute
PPM	: Parts per million
RhB	: Rhodamine B dye (Basic dye)
AAM	: Activated Aegle Marmelos
AAP	: Activated Abrus precatorius
AMC	: Activated Mahua seed carbon
ANC	: Activated Neem Seed carbon

## **INTRODUCTION**

---

Dyes are commonly used in many industries like textile, leather, food, paper, plastics to colour their final products, also in chemical and radiochemical laboratories for analytical purposes. Waste waters emanating from various industries as well as from many biological laboratories are polluted by dyes. Presence of colour and its causative compounds has always been undesirable for both industrial and domestic purpose. More than 8000 types of chemical dye are used in the earth. Dyes are the visible pollutant which mainly pollutes the aquatic life. Every year nearly 1-2 million kg of active dye entering into the biosphere either dissolved or suspended in water. In the dyeing industries, about 30-60 L of water is consumed per kg of cloth dyed and hence large quantities of chemical dye are continuously increasing in our biosphere.

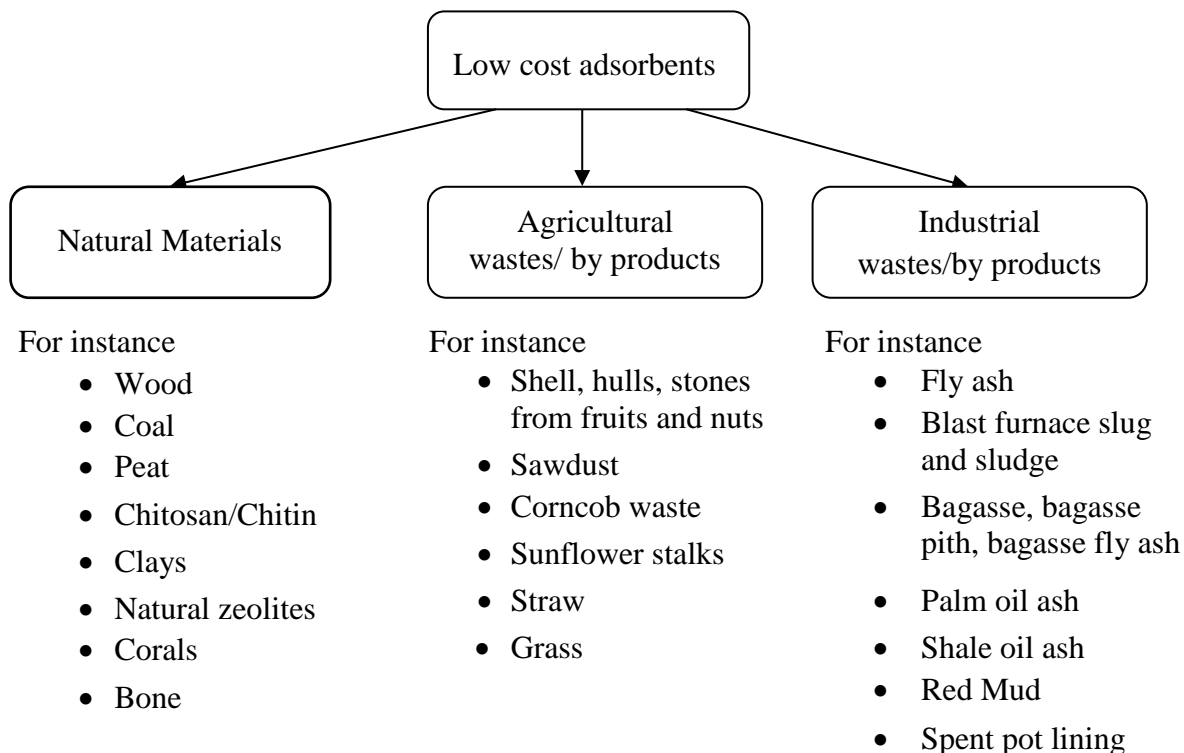
Dyes are known to impart highly obvious color to water which is very undesirable to the water consumer and can deleteriously affect the photosynthetic aquatic life due to reduction of light penetration. Also many dyes and their reaction products, such as aromatic amines are very harmful due to presence of toxic or even carcinogenic groups. Therefore, dyes should be removed from contaminated effluent water before discharge to the environment.

The removal of dye presents a major problem in field of waste water treatment. This is because dye treatment very important, especially those containing an azo group, are highly stable and resistant to heat, light and oxidizing agents. Consequently, they are hard to remove by conventional methods of oxidation or biodegradation. Other procedures, for instance coagulation and flocculation, photo-degradation membrane-filtration processes (Nano-filtration, electro-dialysis, and reverse osmosis etc.) and adsorption can be used for treating dye-containing wastewaters. Of these technologies, adsorption has been preferred to other technologies for removal of dyes from aqueous solutions due to simplicity of the method and ease of manipulation. Various kinds of natural and synthetic adsorbents have been proposed, but adsorption onto activated carbon has gained wide acceptance due to its relatively high capacity and efficiency. Nevertheless, its use is limited due to its high cost and because complete color removal has rarely been achieved with it.

There are many conventional method are their for the treatment with dye effluent are and flocculation (Pans wed& Wongchaisuwan,1986), reverse osmosis (Cohen, 1978) and activated carbon adsorption (Venkata Rao & Sastry, 1987).These technologies do not show

significant effectiveness or economic advantage. Low-cost treatment methods have, therefore, been investigated for a long time.

There is wide range of material for adsorbent preparations. Generally adsorbent's raw material are classified into three categories as (a) Natural material, (b) Agricultural waste/by products, (c) Industrial wastes/ by product.



A number of non-conventional, low-cost adsorbents have been tried for dye removal. These include peat (Poots *et al.*, 1976), wood (Asfour *et al.*, 1985), china clay (Gupta *et al.*, 1989), Fullers earth and fired clay (Mckay *et al.*, 1985), fly ash (Khare *et al.*, 1987), Wollastonite (Singh *et al.*, 1984), Fe(III)/ Cr(III) sludge (Namasivayam & Chandrasekaran, 1991), biogas waste slurry (Namasivayam & Yamuna, 1992; 1992; Yamuna & Namasivayam, 1993; Namasivayam & Yamuna, 1994; 1995; 1995), banana pith (Namasivayam & Kanchana, 1992; 1993; Namasivayam *et al.*, 1993) and waste coir pith (Namasivayam & Kadirvelu, 1994). The present investigation is undertaken to test the use of a cellulosic waste, orange peel, for the removal of different types of dyes: congo red (direct), procion orange (reactive) and rhodamine-B (basic), from water. Orange peel is discarded in the orange-juice and soft-drink industries all over the world. It has been used as an adsorbent for the removal of heavy metals from waste water (Azab & Peterson, 1989). The parameters which affect wastewater treatment, such as dye concentration, agitation time, adsorbent dosage and pH were investigated in batch-mode adsorption studies.

Especially for removal of RhB dye many adsorbents or activated carbon were used like sodium montmorillonite clay[1],Animal Bone Meal[2],Natural perlite[3],Mineral-Catalyzed Fenton[4] , FS300[5] are categorized as a natural type of adsorbent. In the category of preparation of adsorbent or activated carbon from industrial waste for RhB dye removal were Waste slurry[6], Red Mud[7],Oil Palm Empty Fruits Bunch[8],Scrap Tires[9],Waste fruit residues[10],Jack fruit peel[11],Banana And Orange Peels[12],Mustard Cake[13] .

Again another category of adsorbent for the removal of RhB, were used as agricultural waste or by product. Thespusia populinia bark[14],Eichornia Crassipes[15],Almond Shell[16],Palm Shell[17],Mango Leaf Powder[18],Rhizo pusoryzae[19],Photo Catalyst Anatase Titanium Dioxide[20], Cocoa (Theobroma Cacao) Shell[21],Cynodon dactylon[22],Azadirachta indica bark[23], orange peel[24], Jute stick powder[25], Phoenix Sylvestric leaves[26],Wood apple outer shell [27].

## **2.1 ACTIVATED CARBON**

Activated carbon is a porous form of carbon which is manufactured from various carbonaceous raw materials like pine, wood, Coconut shell, Coal, Eucalyptus, peat, Saw dust, Rice husk, Lignite etc.. It is prepared through carbonization and activation of organic substance. During carbonization most of the non-carbon elements like hydrogen, oxygen are first removed in gaseous form and it develops the internal pores and then after it is activated through chemical activation or steam activation. In activation process, it increases the numbers and dimensions of pores and hence it has large internal surface area. Due to well-developed pore structure and huge internal surface area, activated carbon has an excellent adsorbent capacity in both form powder activated carbon and granular activated carbon.

### **Application of activated carbon**

There is a huge application of activated carbon due to its vast application and lost effectiveness and simple way of use. Following are the usual main use of activated carbon

- Effluent Treatment Plant to reduce BOD/COD/Colour from Industrial waste water.
- Purification of drinking water. Air & Gas mask.
- To absorb moisture from compressed Air for paint shop.
- To De-chlorinate soft drink plant process water & swimming pools.
- To remove oil from hot condensate.
- To remove oil vapour from Gas Stream.
- Solvent recovery & Gold recovery.
- Removal of dissolved organic impurities.

- To remove odour.
- Breweries & distilleries.
- Catalyst carrier in Petroleum Refineries.
- Purification of carbon dioxide & Industrial Gas.
- Decolourisation of Plasticizer, Glycerene & fine Chemicals, Dyes Intermediates,
- Pharmaceutical Bulk Drug & Food Colours, Sugar Solutions, Glucose, Dextrose,
- Lactose & other starch sugar solution, (Vegetable oil & fats, Herbal Products).
- Used in Pharmaceutical Formulation, IV Fluid & Laboratory Chemicals, Pesticides & Insecticides Industries.

## **USE OF ACTIVATED CARBON INDUSTRIES**

Activated carbon finds extensive use as a purifier colour adsorbed and deodorizer in these following industries, such as:

- Textile
- Dyes and dye Intermediates
- Active Pharmaceutical Ingredients
- Pharmaceutical Formulations
- Food colors and dyes
- Organic and Inorganic Chemicals
- Petrochemicals
- Oil and gas refinery
- Agrochemicals
- Common Effluent treatment plants
- Drinking water
- Sugar manufacturers
- Starch and Glucose manufacturers
- Environment Consultants

## **OBJECTIVE OF THE PROJECT WORK**

The specific objective of these studies to do proper investigation for adsorptive removal of basic dye ( Rhodamine B) from waste water using self-prepared activated carbon

- i) Preparation of low cost adsorbents with high surface area from biomass/agricultural waste
- ii) Study of different types adsorption and different parameter of adsorption of basic RhB dye
- iii) Comparative study of RhB dye removal by new literature with existing literature
- iv) Characterization of all the adsorbents for their various adsorbable properties such as surface area, proximate , TGA, CHNS, FTIR ,SEM, EDX and XRD
- v) Kinetic, Equilibrium, Adsorption Isotherms, Thermodynamic and optimization based on conventional method

## Literature Review

### 2.1 PRINCIPLE OF ADSORPTION

#### 2.1.1 Adsorption

Adsorption is a process that occurs when a gas or liquid solute accumulates on the surface of a solid or a liquid, forming a molecular or atomic film. In other words, adsorption is the adhesion of atoms, ions, biomolecules or molecules of gas, liquid, or dissolved solids to a surface and this process creates a film of the adsorbate (the molecules or atoms being accumulated) on the surface of the adsorbent. It is a surface phenomenon and a consequence of surface energy. The atoms on the surface of the adsorbent are not wholly surrounded by the other atoms and thus, can attract adsorbate.

Adsorption takes place primarily on the walls of the pores or at specific sites inside the particle. As the pores are generally small, the internal surface area is greater than the external area. Separation occurs because differences in molecular weight, shape or polarity cause some molecules to be held more strongly on the surface than others. In many cases, the adsorbate is held strongly enough to allow complete removal of that component from the fluid, McCabe smith [29].

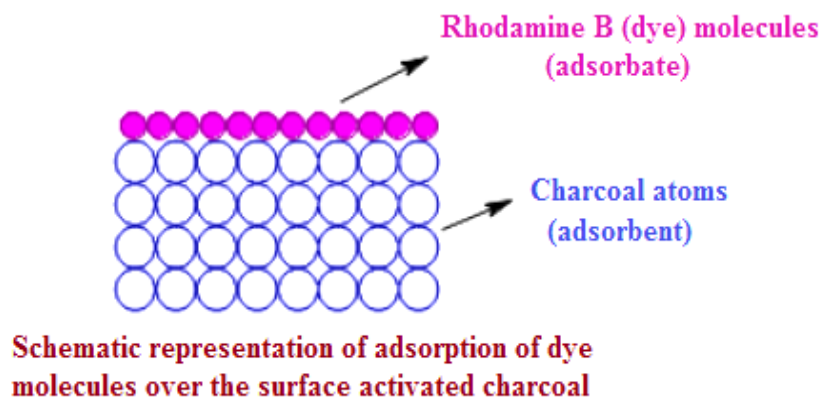


**Figure 2.1:** Schematic representation of adsorption mechanism

#### 2.1.2 Adsorbate

The gas or liquid that is accumulated over the surface of a liquid or solid is known as adsorbate.

#### 2.1.3 Adsorbent

The solid or liquid on whose surface, molecules of other substance are adsorbed. Solids, particularly in finely divided state, have large surface area and therefore act as good adsorbents.

E.g. activated charcoal, silica gel, alumina gel, clay, colloids, metals in finely divided state, etc.

### 2.1.4 Energy of adsorption

The surface atoms or molecules of adsorbent are relatively unstable due to positive surface free energy. Unlike in the bulk, there are unbalanced residual forces at the surface as the molecules at the surface are not symmetrically surrounded by other molecules. Hence they have tendency to attract adsorbate molecules and retain them to minimize the surface energy.

Adsorption is an exothermic process (i.e.,  $\Delta H = -ve$ ) i.e., heat is liberated since new bonds are formed. However entropy of the system is also decreased (i.e.,  $\Delta S_{sys} = -ve$ ) due to decrease in the number of microstates and decrease in the freedom of movement of molecules. Hence adsorption is thermodynamically more favourable at low temperatures.

The value of  $\Delta G$  becomes negative, only at low temperatures, when both  $\Delta H$  and  $\Delta S_{sys}$  are negative. Therefore, in general, at higher temperatures, the bonds between adsorbate and adsorbent are weakened and the reverse of adsorption i.e. desorption is favored.

### 2.1.5 Type of adsorption

Depending on the type of attractions between adsorbate and adsorbent and the exact nature of the bonding depends on the details of the species involved, but the adsorption process is generally classified as follows:

- (1) **Physisorption:** It is a type of adsorption in which the adsorbate adheres to the surface through Van der Waals (weak intermolecular) interactions.
- (2) **Chemisorption:** It is a type of adsorption whereby a molecule adheres to a surface through the formation of a chemical bond.

#### 2.1.5.1 Physical adsorption or physisorption

If the adsorbate molecules are attracted by weak van der Waals forces towards the adsorbent molecules, the adsorption is known as physical adsorption or physisorption.

#### Characteristics of Physisorption

- (i) **Energetics & kinetics:** Physisorption is an exothermic process. However it is characterized by low enthalpy values (20– 40 kJ mol<sup>-1</sup>), due to weak van der Waals forces of attraction. The activation energy for physisorption is also very low and hence it is practically a reversible process.
- (ii) **Effect of temperature:** Since physical adsorption is an exothermic process, it occurs more readily at lower temperatures and decreases with increase in temperature (Le-Chatelier's Principle).
- (iii) **Effect of pressure:** In case of physisorption of gases over solids, the extent of adsorption increases with increase in pressure as the volume of the gases decrease during adsorption (Le-Chatelier's Principle).



(iv) **Specificity:** Since the van der Waals' forces are universal, a given surface of an adsorbent does not show any preference for an adsorbate in physisorption i.e. it is not specific with respect to adsorbent.

(v) **Nature of adsorbate:** However, the extent of adsorption depends on the nature of gas (adsorbate). In general, easily liquefiable gases with higher critical temperatures are readily adsorbed as the van der Waals' forces are stronger, especially, near the critical temperatures.

E.g. Sulphur dioxide (critical temperature 630K) is adsorbed more than methane (critical temperature 190K) over activated charcoal under given set of conditions.

(vi) **Surface area of adsorbent:** The extent of adsorption increases with the increase of surface area of the adsorbent. Hence finely powdered metals and porous substances having large surface areas perform well as adsorbents.

### 2.1.5.2 Chemical adsorption or Chemisorption

If the adsorbate molecules are bound to the surface of adsorbent by chemical bonds, the adsorption is known as chemical adsorption or chemisorption.

#### Characteristics of chemisorption

(i) **Energetics & kinetics:** Chemisorption is also an exothermic process and the enthalpy values are higher ( $80\text{--}240\text{ kJ mol}^{-1}$ ) as it involves formation of chemical bonds. However, the activation energy for chemisorption is high and occurs slowly. Hence it is also called activated adsorption. It is practically irreversible.

(ii) **Effect of temperature:** Even though chemical adsorption is an exothermic process, it does not occur slowly at lower temperature due to high kinetic energy barrier. Hence, like most chemical changes, the extent of chemisorption increases with increase in temperature up to certain limit and then after that it starts decreasing. It is also observed that, in some cases, physisorption of a gas adsorbed at low temperature may change into chemisorption at a high temperature.

(iii) **Effect of pressure:** The chemisorption is not appreciably affected by small changes in pressure. However, very high pressures are favourable for chemisorption.

(iv) **High specificity:** Chemisorption is highly specific and occurs only if there is some possibility of chemical bonding between adsorbent and adsorbate. E.g. Oxygen is adsorbed on metals due to formation of oxide.

(v) **Surface area:** Like physisorption, chemisorption also increases with increase of surface area of the adsorbent.

### 2.1.6 NATURE OF ADSORPTION

Physical adsorption generally is caused mainly by van der Waals force and electrostatic force between adsorbate molecules and the atoms which compose the adsorbent surface. Thus adsorbents are characterized first by surface properties such as surface area and polarity. A large specific surface area is preferable for providing large adsorption capacity, but the creation of a large internal surface area in a limited volume inevitably gives rise to large

numbers of small sized pores between adsorption surfaces. The size of microspore determines the accessibility of adsorbate molecules to the adsorption surface so the pore size distribution of micro pore is another important property for characterizing adsorptivity of adsorbents.

Also some adsorbents have larger pores in addition to micro pores which result from granulation of fine powders or fine crystals into pellets or originate in the texture of raw materials. These pores called macropores are several micrometers in size. Macro pores function as diffusion paths of adsorbate molecules from outside the granule to the micropores in fine powders and crystals. Adsorbents containing macro pores and micro pores are often said to have "bi dispersed" Pore structures.

Surface polarity corresponds to affinity with polar substances such as water. Polar adsorbents are thus called "hydrophilic" and alumino-silicates such as zeolites, porous alumina silica gel or silica-alumina are examples of adsorbents of this type. On the other hand, nonpolar adsorbents are generally "hydrophobic". Carbonaceous adsorbents, polymer adsorbents and silicalite are typical nonpolar adsorbents. These adsorbents have more affinity with oil than water.

## **2.2 Review on Rhodamine B dye removal**

This review is based on adsorptive mode of Rhodamine B (RhB) dye removal from wastewater using activated carbons. Many scientist and researcher did many works for the removal of dye. A briefer view of work by the different researcher is presented. All researcher in the followed papers studied the Physicochemical parameters like dye concentration, solution pH, temperature and contact time have been varied to study the adsorption phenomenon.

- 1. Namasivayam et al., (1991),** had studied the basic dye removal by biogas waste slurry from aqueous solution. Here rate controlling step is mainly intra particle diffusion. Adsorption rate constant was found to be  $0.029 \text{ min}^{-1}$  at 20 mg/l initial dye concentration. They found that the adsorption is following Freundlich isotherm. In the pH range 2.3 to 11.2, dye removal was found at least 90%. Desorption of dye in 50% (v/v) acetic acid to the extent of 69.7% indicate the most dye is held by the chemisorption.
- 2. Namasivayam et al., (1996),** had examined sorption onto the adsorbent prepared from waste orange peel. The adsorption obeyed both Langmuir and freundlich isotherms and the process was following first order rate kinetic. Adsorption capacity was 3.2 mg/g and Acidity pH (=3.0) was favorable for adsorption RhB dye. Desorption studies showed that alkaline pH was efficient for desorption of RB dye.

3. **B. Stephen Inbaraj & N. Sulochana (2005)**, They took the jackfruit peel as agricultural waste, for the removal study of the basic dye, from aqueous solution. Among the isotherm models applied to the equilibrium data Redlich-Peterson model better predicted the experimental values. The adsorption capacity was  $121.47 \text{ mg.g}^{-1}$  at an initial pH of 6.0 and at  $32 \pm 0.5^\circ\text{C}$ . Adsorption capacity increased with increase in temperature. The influence of pH on dye removal was not significant. An optimum carbon dose of  $1.2 \text{ g/L}$  was required for the maximum removal (96%) of dye from its  $60 \text{ mg/L}$  solution. A significant portion of the dye was recovered from the spent carbon using 50% acetic acid.
4. **Sujoy K. Das et al. (2006)**, studies on the removal of a carcinogenic dye rhodamine B (C. I. 45170) from wastewater by biomass of different mould and yeasts is described. Among all of the fungal species tested, the biomass of *Rhizo pusoryzae* MTCC 262 is found to be the most effective. Dye adsorption reaches maximum with the biomass harvested from the early stationary phase of growth. The optimum temperature and pH for adsorption are observed to be  $40^\circ\text{C}$  and 7.0, respectively. The adsorption rate is very fast initially and attains equilibrium after 5 h. The adsorption isotherm follows the Langmuir isotherm model satisfactorily within the studied dye concentration range. Of the different metabolic inhibitors tested, 2,4-dinitrophenol (DNP) and *N,N'*-di-cyclo hexyl carbodiimide (DCCD) decrease dye adsorption by  $\sim 30\%$  suggesting the role of energy metabolism in the process. Spectrophotometric study indicates that the removal of RhB by *R. oryzae* biomass involves an adsorption process. Scanning (SEM) and transmission (TEM) electron microscopic investigations have been carried out to understand the probable mechanism of the dye-biomass interaction.
5. **Hameed et al., (2007)** had investigated the acidic dye removal by using activated carbon from Rubber (*Hevea brasiliensis*) seed coat was used. The equilibrium adsorption data of on activated carbon were analyzed by the Langmuir, Freundlich and Temkin isotherm models. The isotherm data were well described by the Freundlich isotherm model. The monolayer adsorption capacity was  $227.27 \text{ mg/g}$  at  $30^\circ\text{C}$ . Pseudo-first-order; pseudo-second-order and intra particle diffusion models were used to analyze the kinetic data obtained at different concentrations. The adsorption kinetics was well described by the pseudo-second-order kinetic model. Rubber seed coat-based activated carbon was shown to be a promising material for adsorption of from aqueous solutions.
6. **S.Arivoli & M.Thenkuzhali,(2008)**, took *Phoenix Sylvestric* leaves as adsorbent, an indigenous agricultural waste was Sulphuric acid treatment was tested for its efficiency in removing. The adsorption followed first order reaction equation and the rate is mainly controlled by intra-particle diffusion. Freundlich and Langmuir isotherm models were

applied to the equilibrium data. The adsorption capacity,  $Q_m$  obtained from the Langmuir isotherm plots were 51.546, 47.236, 44.072 and 41.841 mg/g respectively at an initial pH of 7.0 at 30, 40, 50 and 60 °C. The temperature variation study showed that the adsorption is endothermic and spontaneous with increased randomness at the solid solution interface. Significant effect on adsorption was observed on varying the pH of the solutions. Almost 90% removal of was observed at 60 °C. The Langmuir and Freundlich isotherms obtained, positive  $\Delta H^0$  value, pH dependent results and desorption of dye in mineral acid suggest that the adsorption of on PSC involves physic sorption mechanism.

7. **M. Hema& S. Arivoli,(2009)** were studied on effective removal of using acid treated carbonaceous *Thespusia populinia* bark adsorbent. Freundlich and Langmuir isotherm plots were 60.836, 64.239, 68.695 and 77.178 mg/g respectively at an initial pH of 7.0 at 30°,40°, 50° and 60° C. The temperature variation study showed that the RB adsorption is endothermic and spontaneous with increased randomness at the solid solution interface. Significance effect on adsorption was observed on the varying the pH of the RB solution .Almost 79% removal of was observed at 60° C .The Langmuir and freundlich isotherms obtained, positive  $\Delta H^0$  value, pH dependent results and desorption of dye in the mineral acid suggest that the adsorption of RB on adsorbent involve physisorption mechanism.
8. **Panda et al.,(2009)**, took Jute stick powder (JSP) as promising material for adsorptive removal of RhB dye from aqueous solutions.. Favorable adsorption occurs at around pH 7.0 whereas temperature has no significant effect on adsorption of both the dyes. The maximum adsorption capacity has been calculated to be 87.7 mg/g of the biomass for .The adsorption process is in conformity with Freundlich and Langmuir isotherms for .Adsorption occurs very fast initially and attains equilibrium within 60 min. Kinetic results suggest the intra-particle diffusion of dyes as rate limiting step.
9. **Xu H Y et al.(2009)**,has studies on natural iron-bearing minerals, schorl could be taken as an effective iron source for degradation of organic pollutants by mineral-catalyzed Fenton-like system. In our present study, the schorl-catalyzed Fenton-like system has been successfully developed for discoloration of an active commercial dye, Rhodamine B (RhB), in an aqueous solution. Through a number of batch discoloration experiments under various conditions, it was found that the reactivity of the system increased by, respectively, increasing schorl dosage, temperature, hydrogen peroxide starting concentration and by decreasing the pH. Over 90% of discoloration ratio could be gained in less than 30 min, and nearly 70% of total organic carbon (TOC) could be removed in less than 200 min. And, the schorl catalyst could be repeatedly used at least ten times, still with high catalytic activity. Comparative studies indicated that the RhB discoloration

ratios were much higher in presence of schorl and  $\text{H}_2\text{O}_2$  than those in presence of schorl or  $\text{H}_2\text{O}_2$  only, which suggested that the schorl-catalyzed Fenton-like reaction governed the RhB discoloration process. The content of Fe ion leaching in the solution was also measured using inductively coupling plasma-atomic emission spectra (ICP-AES). A mechanism proposed herein suggested that adsorption and Fenton-like reaction (heterogeneous and homogeneous) were responsible for the discoloration of RhB.

10. **Rajeshwari Sivaraj et. al. (2010)**, studied on the ability of the activated carbon prepared from *Eichornia Crassipesto* remove Reactive Magenta B and Reactive Turquoise Blue dyes from aqueous solution has been carried out as a function of contact time, dose (0.1-0.60 mg/50ml for Magenta B and 0.25-2.0 mg/50ml for Turquoise Blue), pH (2-10) and concentration (25, 50, 75, 100mg.L<sup>-1</sup>). An amount of 0.6 g of the adsorbent could remove 56.0% of the dye from 100mg.L<sup>-1</sup>.Magenta B dye solution and 2.0 g could remove 45.87% of Turquoise Blue dye from 100 mg.L<sup>-1</sup>.Turquoise Blue dye solution. The amount of dye adsorbed per unit weight of the adsorbent increased from 15.64 to 56.01 mg.g<sup>-1</sup> with increasing concentration from 25 to 100 mg.L<sup>-1</sup>. The kinetics of adsorption was discussed in view of the kinetic models, the pseudo-first-order Lagergren model, Langmuir, Freundlich, Tempkin, Harkin's-Jura, Elovich and the pseudo-second-order model.
11. **Maedeh Mohammadi et al.(2010)**,did research on Palm shell derived activated carbon was utilized as a potential adsorbent to remove RhB dye from aqueous solution. Activated carbon was prepared from palm shell through a physiochemical activation process to yield a sample with a Brunauer-Emmett-Teller (BET) surface area of 476.8 m<sup>2</sup>.g<sup>-1</sup>. The ability of the prepared activated carbon for dye adsorption was examined in a series of batch experiments. The effect of various process parameters such as initial dye concentration (41.8 to 208.8)  $\mu\text{mol} \cdot \text{L}^{-1}$ , solution pH (3 to 11), and temperature [(30 to 50) °C] on the adsorption capacity of the adsorbent was investigated. Various adsorption isotherms (Langmuir, Freundlich, and Temkin) were used to interpret the experimental data. The obtained sorption data were reasonably described by the Langmuir model. The Temkin isotherm confirmed the presence of a repulsive lateral interaction in the adsorbent surface. Pseudo first- and second-order kinetic models were used to predict the kinetics of the adsorption process. The obtained results revealed that the adsorption of RB on activated carbon followed a pseudo second-order kinetic model. A maximum dye removal efficiency of 95 % was achieved at an initial dye concentration of 62.6  $\mu\text{mol} \cdot \text{L}^{-1}$ , pH = 3, and temperature of 50 °C.

12. **Li Li et al., (2010)**, Activated carbon derived from solid hazardous waste scrap tires was evaluated as a potential adsorbent for cationic dye removal. The adsorption process with respect to operating parameters was investigated to evaluate the adsorption characteristics of the activated pyrolytic tire char (APTC) for Rhodamine B (RhB). Systematic research including equilibrium, kinetics and thermodynamic studies was performed. The results showed that APTC was a potential adsorbent for RhB with a higher adsorption capacity than most adsorbents. Solution pH and temperature exert significant influence while ionic strength showed little effect on the adsorption process. The adsorption equilibrium data obey Langmuir isotherm and the kinetic data were well described by the pseudo second-order kinetic model. The adsorption process followed intra-particle diffusion model with more than one process affecting the adsorption process.
13. **C. Theivarasuet. al.(2010)**, removes the Rhodamine-B (RB) from aqueous solutions by cocoa (*Theobroma cacao*) shell activated carbon (CSAC) was studied in a batch adsorption system. The adsorption studies include both equilibrium adsorption isotherms and kinetics. The adsorption equilibrium was represented with Langmuir, Freundlich, Tempkin, Harkin's - Jura and Dubinin-Radushkevich isotherm models. Pseudo first order, pseudo second order, Elovich and Intraparticle diffusion kinetic models were used to test the adsorption kinetics. The kinetic data were well described by the pseudo second order kinetic model. The mechanism of the adsorption process was determined from the intraparticle diffusion model. The results indicated that CSAC could be employed as a low cost alternative for the removal of RB from diluted industrial effluents.
14. **Gupta et al.,(2010)**, studied on removal of sorption from wastewater effluent. Therefore Mustard cake, obtained from local oil mills, has been characterized and used as an inexpensive and effective adsorbent. The influence of various factors on the adsorption capacity has been studied by batch experiments. The optimum contact time to reach equilibrium was found to be 6 h. Maximum decolorization took place at pH 2.30. The optimum adsorbent dose was 5 g.L<sup>-1</sup> of particle size < 106  $\mu$ m. The ongoing adsorption validates both the Langmuir and the Freundlich adsorption isotherms at temperatures of (40, 50, and 60) °C. Thermodynamic parameters indicate the feasibility of the process. The desorption profile revealed that a significant portion (80 %) of RB dye could be desorbed by using 50 % ethanol as eluting agent. Desorption studies indicated the possibility of recycling and regeneration of both the adsorbent and the dye
15. **Ahamed et al.,(2011)**, took carbonaceous adsorbent which were prepared from an agricultural waste, Azadirachta indica bark (AIC), by acid treatment was tested for its efficiency in removing RhB dye. Freundlich and Langmuir isotherm models were applied

to the equilibrium data. The adsorption capacity,  $Q_e$  obtained from the Langmuir isotherm plots with temperature variation study showed that the RB adsorption is endothermic and spontaneous with increased randomness at the solid solution interface. Significant effect on adsorption was observed on varying the pH of the RhB solutions. Almost 94% removal of RhB was observed at 50 °C. Thermodynamic parameters such as  $\Delta H^\circ$ ,  $\Delta S^\circ$ , and  $\Delta G^\circ$  were evaluated. The positive  $\Delta H^\circ$  value, pH dependent results and desorption of dye in mineral acid suggest that the adsorption of on AIC involves physisorption mechanism.

**16. P. Parimaladevi & V. Venkateswaran, (2011),** studies on adsorbent prepare from fruit waste digested with phosphorous (V) oxy chloride (PFR) for RhB removal. Behavior of adsorption followed pseudo second order kinetics and the rate is mainly controlled by intra particle diffusion. Langmuir and Freundlich models were applied to the equilibrium data. The adsorption capacity ( $Q_e$ ) obtained from the Langmuir isotherm plots at 302K were 34.48 mg/g and 35.71 mg/g respectively at pH of 7.1 and 6.2. The temperature variation study showed that the adsorption is endothermic and spontaneous with increased randomness at the solid solution interface. By varying the pH of the dye solution significance effect on adsorption was observed. Langmuir and Freundlich isotherms obtained, positive  $\Delta H^\circ$  value, pH dependent results and poor desorption of indicated that adsorption of these dyes on PFR involved chemisorption mechanism.

**17. Haddad et al, (2012),** studied the adsorptive removal of a cationic dye, RhB from aqueous solutions was achieved by the use of Animal Bone Meal as a new low cost adsorbent. Adsorption of RhB Dye was occurred by studying the effects of contact time, adsorbent amount, dye concentration and temperature. Dye adsorption equilibrium was rapidly attained after 60 minutes of contact time. The isotherms of adsorption data were analyzed by the Langmuir and Freundlich adsorption isotherm models. The adsorption capacity ( $Q_m$ ) obtained from Langmuir isotherm plots were 62.11, 63.69, 64.13 and 64.95 mg/g respectively at 303, 313, 323 and 333°K. Thermodynamic parameters such as  $\Delta H^0$ ,  $\Delta S^0$  and  $\Delta G^0$  were calculated, which indicated that the adsorption was spontaneous and endothermic nature. The characteristic results and dimensionless separation factors  $R_L$  showed that animal bone meal can be employed as an alternative to commercial adsorbents in the removal of RhB dye from aqueous solution and wastewater.

**18. Vijaya kumar et al. (2012),**In this paper, they studied the feasibility of removal of basic dye RhB from aqueous solutions by using a low cost natural adsorbent perlite. Batch adsorption experiments were carried out as a function of pH, contact time, initial concentration of the adsorbate, adsorbent dosage and temperature. Dye adsorption

equilibrium was rapidly attained after 50 minutes of the contact time, and it was described by the Langmuir and Freundlich adsorption isotherms over the entire concentration ranges from 20-100 mg.L<sup>-1</sup>. Adsorption data's are used for modeling, from the first and second order kinetic equation and intra-particle diffusion models. Thermodynamic parameters such as  $\Delta H^0$ ,  $\Delta S^0$ , and  $\Delta G^0$  were calculated, which indicated that the adsorption was spontaneous and exothermic nature, which was evident by decreasing the randomness of the dye at the solid and liquid interface. Adsorbent used in this study, characterized by FTIR and SEM before and after the adsorption of RhB. The characteristic results and dimensionless separation factors ( $R_L$ ) showed that perlite can be employed as an alternative to commercial adsorbents in the removal of RhB from aqueous solution and wastewater.

19. **Majid Aliabadi et al.(2012)**, had studied the adsorption using almond shell (*Prunusdulcis*) biosorbent has been investigated to remove the RhB from aqueous solutions. Almond shell has been selected as an adsorbent because of advantages such as high adsorption capacity, nontoxicity, availability and low cost. The effects of contact time, initial dye concentration, adsorbent dosage, particle size and solution pH were studied. The results showed that the removal efficiency increased by increasing contact time, adsorbent dosage and initial dye concentration. In addition, the adsorption was dependent to solution pH and the maximum adsorption was observed at a solution pH of 2.0. The Langmuir, Freundlich and Temkin isotherms were used to describe the adsorption equilibrium data. Freundlich equation fits the experimental data better than the Langmuir and Timken equations do.
20. **B.R. Venkatraman et al. (2012)**, Here RhB adsorption from an aqueous solution onto acid activated Cynodon dactylon carbon has been studied experimentally using batch adsorption method. Adsorption Kinetics and equilibrium were investigated as a function of initial dye concentration, pH, contact time, and adsorbent dosage. Kinetic studies indicated that the adsorption followed reversible First order reaction. Equilibrium data was analyzed using Langmuir and Freundlich isotherm models. The adsorption capacity of Cynodon dactylon was found to be 94 % on the basis of experimental results and the model parameters, it can be inferred that the carbonaceous Cynodon dactylon is effective for the removal of RhB from aqueous solution.



## MATERIAL AND METHOD

### 3.1 MATERIALS

All the required reagents used throughout the project were A.R. grade and procured from Rankem chemicals and Merck chemicals. Filtration purpose Whatman filter paper of size 40 $\mu$ m and syringe and micro filterate syringe filter of Whatman 0.45 $\mu$ m were used. The Adsorbents selected for the adsorption studies of Rhodamine B (RhB) dye procured from Merck chemicals. Stoke Solution of the dye prepared by weighting out the pure powder form solids dye. Four different agricultural waste biomass was collected from locality of Rourkela.

### 3.2 INSTRUMENTS

Throughout the project no. of instruments were used, which were made the analysis quicker and easier. The supernatant concentration of dye solution was determined by using previously prepared calibration curve at characteristics wavelength  $\lambda_{\max} = 540$  nm, using UV-Visible spectrophotometer which was combined with a computer (*JASCO, V-530, Samsung system*).

**Table 3.1:** Details of instruments used during the research work

Instrument Name	Company Name/Model No.
UV-Visible Spectroscopy	JASCO, V-530
pH meter	SYSTRONICS , $\mu$ pH System 360
Shaker	REMI ELEKTRONIK LTD.
Weight Machine	Denver Instrument ,SI-234
BET analysis	Quantachrome Autosorb Automated Gas Sorption System
Ultimate Analysis	Vario EL Cube CHNS Analyzer, Elementar CHNSO
SEM	JEOL
FTIR	SHIMANDZU IR PRESTIGE-21

REMI's hot water bath shaker was used for shaking purpose up to 6 hours with high temperature and it has 12 holders for holding the 100 ml conical flask size glassware .Hot air oven used for each time for drying purpose. Sieve analysis was done with the help of BSS (British Standard Scale) types of sieves with mesh size Numbers were 16, 18, 20, 25, 30, and 35. Among all mesh sizes maximum quantity of powdered achieved in 30 mesh size (500 $\mu$ m) and selected as regular adsorbent particle size for whole experiments.

### 3.3 ADSORPTION DEPENDS UPON SEVERAL FACTORS

There are several factors on which the effectiveness of adsorption process depends upon these adsorption conditions which may either be the nature of the adsorbent (acidic/ basic) or the characteristics of adsorbent which includes the high surface area, pore size distribution, ash content and hydrophobicity.

The acidity or basicity of the activated carbon depend upon the presence of hetero atom's such as oxygen, which can form phenols, ethers, lactones ketone, carboxyl and nitrogen in the form of amines and nitro groups; and phosphorus as a phosphate can determine.

On the other hand, adsorption also depends on the nature of the adsorbate depends on its hydrophobicity, polarity, and size of the molecule.

In search of alternative of commercial Activated carbon, low cost adsorbent are investigated. Broadly, the raw materials used for the preparation of novel adsorbents are classified under three main categories: Agricultural Waste (AW) Industrial Waste (IW) Mineral Waste (MW).

### 3.4 ADSORBENT PROPERTIES

The activated carbon prepared from biomass, used for adsorption process. Here four different materials are used for preparation of adsorbent and their characterizations are done.

#### 3.4.1 PHYSICO-CHEMIAL PREPERTIES OF SORBENT

Density, Porosity, Specific gravity, bulk density and dry density were determined with the help of specific gravity bottle of 50 ml capacity using following equations

$$\begin{aligned}\text{Specific Gravity} &= \frac{\text{Weight of sample}}{\text{Weight of equal volume of water}} \\ &= \frac{(W_2 - W_1)}{[(W_4 - W_1) - (W_3 - W_2)]}\end{aligned}\quad (3.1)$$

$$\text{Bulk Density (v)} = \frac{\text{Weight of density bottle + Sample}}{10 \text{ mL}} \quad (3.2)$$

$$\text{Dry Density (v}_d\text{)} = \frac{\text{Bulk Density (v)}}{1 + W} \quad (3.3)$$

Where,

$W_1$  = Weight of the empty density bottle

$W_2$  = Weight of the (density bottle + 1 gm of the sample)

$W_3$  = Weight of the (density bottle + 1 gm of the sample+ water)

$W_4$  = Weight of the (density bottle + water)

$W_5$  = Water content of the sample

Void Fraction (e) and porosity of adsorbents were calculated by using Equations

$$\text{Void Ratio (e)} = \left( \frac{\text{Sp. gravity of sample} \times \text{sp. gravity of water}}{\text{Dry Density (v}_d\text{)}} \right) - 1 \quad (3.4)$$

$$\text{Porosity} = \left( \frac{e}{1 + e} \right) \quad (3.5)$$

Table 3.2 : Physico-chemical properties of adsorbent				
Properties	Activated Aegel mermelos (Bael)	Activated Mahua carbon	Activated Neem Carbon	Activated Abrus precatorius Carbon
Specific gravity	0.997	0.973	0.977	1.0003
Bulk density, g/ml	3.850	3.851	3.852	3.851
Dry density	1.823	1.464	1.437	0.615
Void ratio	0.453	0.336	0.321	0.627
Porosity	0.829	0.506	0.471	0.385

### 3.4.2 pH

The pH of bio-char was determined according to Novak et al. [36] and Cheng and Lehmann [33]. Two grams of bio-char were shaken (*REMI*) with 40 mL distilled water or 1 M KCl (99% of purity Merck Chemicals Ltd.) solution for 30 min. This suspension was allowed to stand for 10 min before measuring the pH with a pH electrode.

The pH of char sample was determined in both water and KCl solutions. For the measurement pH in water, 40 ml of water taken in conical flask and adsorbent of 1gm in added to in the solution of water and kept the dispersed solution in shaker for 1 hours for proper mixing. Initial pH and final pH was measured, after addition of adsorbent change in pH, is due to surface chemical property. Similarly with 0.1 M KCl , pH was measured .In 40 ml of 0.1 M KCl , 1gm of adsorbent putted and kept in shaker for 1 hours .

Table 3.3 : pH measurement Results

Name of sample	Initial pH (with water)	Final pH (with Water)	Initial pH (with KCl)	Final pH (with KCl)
Aegel mermelos Shell	5.93	4.82	6.30	4.37
Neem Seed	6.01	6.39	6.30	5.7
Mahua Seed	6.0	5.05	6.30	4.68
Abrus Precatorius	6.01	5.79	6.30	5.45

### 3.4.3 BOEHM TITRATION

Surface acidity and alkalinity using Boehm titration method Boehm titration provides an indication of the total surface acidity and alkalinity of the bio char, and is based on the method described by Cheng and Lehmann [34]. A 0.15 g subsample of bio-char was added to 15 mL of either 0.1 M NaOH or 0.1 M HCl solutions (Merck Chemicals Ltd.) and shaken with an end-over-end shaker for 30 h. The bio-char slurry was then filtered using a Whatman no. 40 filter paper. An aliquot of 5 mL of the NaOH filtrate was transferred to a 10 mL 0.1 M HCl solution that neutralized the unreacted base. The solution was back-titrated with 0.1 M NaOH with a phenolphthalein indicator. Surface basicity was measured similarly to the measurement of surface acidity and an aliquot of 5 mL of the HCl filtrate was directly titrated with 0.1 M NaOH. The base or acid uptake of BC was converted into the content of surface acidity or surface basicity ( $\text{m.mol g}^{-1}$ ), respectively.

### 3.5 RAW MATERIAL FOR ADSORBENT PREPARATION

We took four different biomass for the preparation of activated carbon by following common method of activation, chemical method. For better comparison of adsorption mechanism, the choosing of four very different materials is important. Activated carbon, prepared from this different biomass is depended upon the nature of construction and chemical formation [6, 8, 10, 11, 41, 42].

#### (I) *Madhuca longifolia* (Mahua Seed)

*Madhuca longifolia*, commonly known as mahwa or mahua, is an Indian tropical tree found largely in the central and north Indian plains and forests. It is a fast growing tree that grows to an height of approximately 20 meters, possesses evergreen or semi-evergreen foliage, and belongs to the family Sapotaceae. It is adapted to arid environments, being a prominent tree in tropical mixed deciduous forests in India in the states of Chhattisgarh, Jharkhand, Uttar Pradesh, Bihar, Maharashtra, Kerala Madhya Pradesh, Gujarat and Orissa.

**Table 3.4:** Scientific Classification of *Madhuca longifolia* seed

Kingdom		Plantae
Order	:	Ericales
Family	:	Sapotaceae
Genus	:	<i>Madhuca</i>
Species	:	<i>M. longifolia</i>



a. Mahua tree with seeds and flowers



b. Raw dried Mahua Seed



c. Carbonized Mahua Seed



d. Activated Mahua carbon of 500 µm

**Figure 3.1:** Systematic preparation of Seed to Activated Carbon of *Madhuca longifolia*

## (II) *Aegle marmelos* ( Bael fruit)

*Aegle marmelos* also known as Bengal quince, stone apple is a species of india native. The bael fruit has a smooth, woody shell with a green, gray, or yellow peel. It takes about 11 months to ripen on the tree and can reach the size of a large grapefruit or pomelo, and some are even larger. The shell is so hard it must be cracked with a hammer or machete. The fibrous yellow pulp is very aromatic. It has been described as tasting of marmalade and smelling of roses. Numerous hairy seeds are encapsulated in aslimy mucilage.

**Table 3.5:** Scientific Classification of *Aegle Marmelos* seed

Kingdom	Plantae
Order	: Sapindales
Family	: Rutaceae
Subfamily	: Aurantioideae
Tribe	: Clauseneae
Genus	: <i>Aegle</i>
Species	: <i>A. marmelos</i>



a. Bael fruit Shell



b. Crushed Raw Bael fruit shell



c. . Dried and crushed Bael Shell



d. Carbonized crushed Bael fruit Shell



e. Activated Bael fruit Shell Carbon



f. Activated Bael shell carbon canister

**Figure 3.2:** Systematic pictorial preparation of Bael Shell to Activated Bael Carbon

### (III) *Azadirachta indica* (Neem) Seed

This plant commonly known as Neem in south Asia region. The fruit is a smooth (glabrous) olive-like drupe which varies in shape from elongate oval to nearly roundish, and when ripe are 1.4–2.8 cm. (0.55–1.1 in) by 1.0–1.5 cm (0.39–0.59 in). The fruit skin (exocarp) is thin and the bitter-sweet pulp (mesocarp) is yellowish-white and very fibrous. The mesocarp is 0.3–0.5 cm (0.12–0.20 in) thick. The white, hard inner shell (endocarp) of the fruit encloses one, rarely two or three, elongated seeds (kernels) having a brown seed coat.



**Table 3.6:** Scientific Classification of *Azadirachta indica* seed

KINGDOM		PLANTAE
Division	:	Magnoliophyta
Order	:	Sapindales
Family	:	Meliaceae
Genus	:	<i>Azadirachta</i>
Species	:	<i>A. indica</i>



a. Neem tree with fruits/seed



b. Raw neem fruit in a branch



c. Well washed Neem seed



d. Activated Neem seed carbon

**Figure 3.3:** Systematic preparation of raw seed to Activated *Azadirachta indica* seed

#### (IV) *Abrus Precatorius* (Crab's Eye) Seed

This is a bio-seed of *Abrus Precatorius* commonly known as Gunja, Jequirity, Crab's Eye, Rosary Pea, John Crow Bead, Precatory bean, Indian Licorice, Akar Saga, Giddee Giddee or Jumbie Bead in Trinidad & Tobago is a slender, perennial climber that twines around trees, shrubs, and hedges. This plant is a legume with long, pinnate-leafleted leaves and its seed are red in colour with a black spot at base of seed.

**Table 3.7:** Scientific Classification of *Abrus Precatorius* seed

Kingdom		Plantae
Order	:	Fabales
Family	:	Fabaceae
Genus	:	<i>Abrus</i>
Species	:	<i>A. precatorius</i>

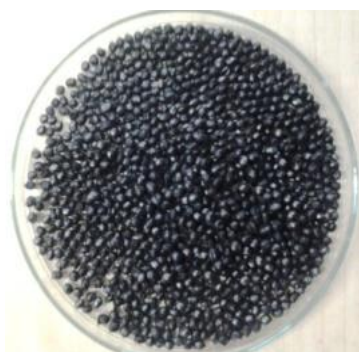


**a.** *Abrus precatorius* plant climbed into a tree

**b.** Plant of *abrus precatorius*



**c.** Seed of *abrus precatorius*



**d.** Carbonized *Abrus* seed



**e.** powdered activated APC

**Figure 3.4:** Systematic preparation of raw Seed to Activated *Abrus Precatorius* seed Carbon

The raw seeds contain abrin, a ribosome inactivating protein that is one of the deadliest plant toxin known; despite their toxicity. Boiled seeds are ingested as a contraceptive and an aphrodisiac. They are also made into a decoction for use as a diuretic, for sore throat and for rheumatism. The seeds are powdered and taken as a snuff for headache; a poultice of the leaves is said to remove freckles; a decoction of the leaves and roots is used for cough, colds, and colic.

### 3.5.1 Steps of adsorbent Preparation:

Preparation of activated carbon is done differently, i.e. one after another material.



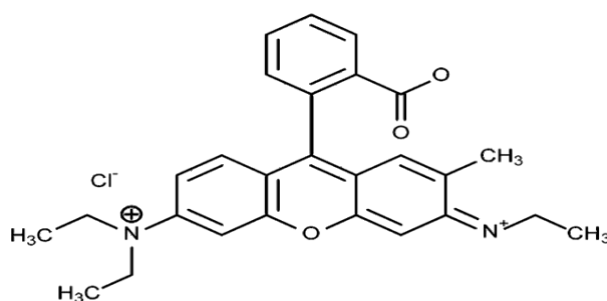
First, Raw material ( Mahua seed, Bael shell, Abrus Precatorius seed and Neem seed) were washed 2 to 3 times with general pipe water for removal of mud ,dust and unwanted external materials

- i. Use single distilled water for second time washing purpose, then dried the material up to 70°C to 90°C for 1hr.
- ii. The dried material transfer into the pyrolytic reactor and reactor put inside the furnaces, by maintaining 370°C for Mahua seed, 390°C temperature for Aegle marmelos, 400°C for Neem seed and 450°C for Abrus precatorius.
- iii. After pre-carbonized of material ,material crushed into powder or granular form using hand blender
- iv. After blending of carbonaceous material, we sized it with the help of sieving technique by taking different size of sieve and choose the 30 BSS (British Standard Scale) sieve which was 500 micron size as our particle size.
- v. Resulting sample is washed with distilled water and unwanted material gets separated as waste filtrate.
- vi. Properly washed carbonized carbon is impregnated with 40% diluted H<sub>3</sub>PO<sub>4</sub>acid solution with an impregnated ratio (W/W) of 4:1 for nearly 20 hours.
- vii. Resulting chemically acid washed Activated Carbon was again washed with single distilled water continuously up to a constant pH reached.
- viii. Finally the washed AC is kept in the oven at 110°C for 3hrs for removal of moisture.
- ix. Dried activated adsorbent kept in plastic storage bottle container for further use.

### 3.6 ADSORBATE

#### 3.6.1 Rhodamine B (RhB) dye

Among the various classes of dyes, basic dyes are the brightest class of soluble dyes used by the textile industry, as their tinctorial value is very high. Rhodamine B is a basic dye by nature. RHB is a basic dye which is widely used in textile, trace, biological laboratory purpose. RHB is a red dye used to dye wool, silk and tannin mordant cotton.



(Rhodamine B)

**IUPAC Name:-** (9-(2-carboxyphenyl)-6-diethylamino-3-xanthenylidene]-diethylammonium chloride)

**Common Names:** Rhodamine B, Rhodamine 610, C.I. Pigment Violet 1, Basic Violet 10

In addition to its application in dyeing industries RB in combination with auramine-O (a basic dye) is used as a biological stain widely in many biomedical research laboratories and as well as in the dyeing of leather and paper. These stains are known to be toxic to human and animals. Though the volume of stain solutions used in these laboratories is relatively small, high concentration of dyes in them results in the formation of waste waters characterized by their toxicity, low transparency of light and high content of organic load.

#### 3.6.1.1 Physical properties of adsorbate (Rhodamine B dye)

<b>Table 3.8 : Physical Properties of adsorbate</b>	
<b>Properties</b>	<b>Rhodamine B ( dye )</b>
Chemical formula	$C_{28}H_{31}ClN_2O_3$
Common Chemical Name	Rhodamine B, Rhodamine-540, Basic Violet 10
IUPAC Name	(9-(2-carboxyphenyl)-6-diethylamino-3 xanthenylidene]-diethyl ammonium chloride)
Molecular Mass (g/mole)	479.02
Melting Point ( $^{\circ}C$ )	210-211 $^{\circ}C$
Vapor pressure (mm Hg at 20 $^{\circ}C$ )	100 k Pa
Solubility in Water (g/L) at 20 $^{\circ}C$	50 g/L
Soluble in organic	Soluble in <u>acetic acid</u> solution (30 vol.%) ~ 400 g/L
Nature	Powder form
CAS No.	81-88-9

### 3.7 Principles of Colour Chemistry

Unlike most organic compounds, dyes possess colour because they 1) absorb light in the visible spectrum (400–700 nm), 2) have at least one chromophore (colour-bearing group), 3) have a conjugated system, i.e. a structure with alternating double and single bonds, and 4) exhibit resonance of electrons, which is a stabilizing force in organic compounds. When any one of these features is lacking from the molecular structure the colour is lost. In addition to chromophores, most dyes also contain groups known as auxochromes (colour helpers), examples of which are carboxylic acids, sulfonic acid, amino, and hydroxyl groups. While these are not responsible for colour, their presence can shift the colour of a colourant and they are most often used to influence dye solubility. The relationships between wavelength of visible and colour absorbed/observed. Regarding the requirement of a chromophore generating colour in organic compounds, it is important to note that the chromophore must be part of a conjugated system.

#### 3.7.1 Importance of having a chromophore within a conjugated system

In addition to influencing solubility, auxochromes are essential ring substituents in providing target colours. This is illustrated in Figure 6, where the following effects of substituents are

shown: Adding groups of increasing electron-donating ability to the azo benzene structure has a bath chromic effect (*cf.* OH vsNH<sub>2</sub>).

- Electron-donating (NH<sub>2</sub>) and electron-accepting (NO<sub>2</sub>) groups placed in conjugation provide a bath chromic effect. In this regard, nitro groups are especially beneficial, contributing to their prevalence in disperse dye structures.
- Increasing the number of electron-attracting groups conjugated with the electron donor has a bath chromic effect.
- The electron-donating effects of an amino group are enhanced by adding alkyl groups to the N-atom.

### **3.8 Preparation of Standard Stoke Rhodamine B (dye) Solution**

Accurately 1gm of powder dye was dissolved in 1000ml of distilled water container. Initially, in one liter measuring flask little quantity less than of single distilled water taken and mixed the weighted 1gm of powder RhB dye in it. Then the dye solutions had shaken thoroughly. Finally single distilled water was poured up to the one liter mark of measuring flask. The stoke solution prepared was 1000mg.L<sup>-1</sup> with single distilled water and next lower concentration prepared by subsequent dilution. The supernatant dye solution was analysis with  $\lambda_{\text{max}} = 540 \text{ nm}$  using JEOL UV-Visible Spectrophotometer.

#### **3.8.1 Analytical measurement of Rhodamin B dye**

The standard calibration curve of known concentrations of RhB dye was plotted by finding out the absorbance at the characteristic wavelength of  $\lambda_{\text{max}} = 540\text{nm}$ . A spectrophotometer (JEOL UV/Vis-530) was used for the calibration plot, which showed a linear variation of absorbance up to 30 mg/L concentration. Therefore, the samples with higher concentration above 10ppm (mg/L) of dye were diluted by 5 or 10 times with distilled water.

### **3.9 ADSORPTION STUDIES**

#### **3.9.1 EXPERIMENTAL METHODOLOGY USED FOR THE ADSORPTION**

Many researchers investigated by following several methods and techniques to stimulate the intimate contact between adsorbent and adsorbate for the maximum up taking of pollutant from aqueous medium. Initially calibration curve done before adsorption studies to generate the equation, which implies absorbance is the function of concentration.

Broadly, adsorption studies done in *batch contact system* method or *continuous flow system* method. Here all the studies of optimized operational variables done in *batch contact system* method. For all experiments including the adsorption Kinetics, isotherms, thermodynamics, were determined by batch method which easy and simple to execute.

### 3.10 BATCH CONTACT SYSTEM ADSORPTION STUDIES

Generally in batch contact process, graphically determined amount of adsorbent is agitated with a specific volume of adsorbate solution having known concentration for a certain period of time until the concentration of adsorbate in solution phase decrease to a desirable level. The removal rate of adsorbate mainly depend upon the force of driving the rate of the adsorption and solution concentration as physical parameters and surface area, porosity .of adsorbent as morphological parameters, acidity or basicity nature of adsorbent also important parameters. Preliminary experimental done to optimize the adsorbent dose and agitation time. In the present studies, a series of batch adsorption experiments were conducted to determine the adsorption of Rhodamine B on Activated Mahua Carbon (AMC) and Activated Neem Carbon (ANC). All the batch adsorption experiments were performed in a mechanical shaker equipped with a thermostatic water bath at constant speed of 120 rpm using 100 ml conical flasks with stopper containing 50 ml each of dye solutions of 100 ppm concentration. Experiments were performed at room temperature of 27 °C (300 K). The pH of the solution was maintained natural as well as desire done when needed likewise the other parameters such as adsorbent doses, temperature, contact time were also either varied or kept at desired level as per the need. All solution samples post adsorption were filtered through syringe driven Millipore Whatman (0.45µm) filter sockets. The concentrations of dye in treated samples were determined by UV spectrophotometer and by comparing with calibration equation

The amount of dye adsorbed per unit mass of the adsorbent was evaluated by using the following equation,

$$Q_t = \frac{C_0 - C_t}{M} \times V \dots\dots\dots(3.6)$$

Where,        Co = Initial Concentration of dye, 100 ppm (mg/L)  
                   C<sub>t</sub> = Liquid phase concentrations of dye at any time(in mg/L)  
                   V = Volume of dye took for adsorption, in ml  
                   M = Weight of adsorbent dose, in gram

$$Q_e = \frac{(C_0 - C_e)}{M} \times V \dots\dots\dots(3.7)$$

Where,        Co = Initial Concentration of dye, 100 ppm (mg/L)  
                   C<sub>e</sub>= Liquid-phase concentrations of dye at equilibrium

The percentage removal of RHB dye was calculated by the following equation,

$$\% \text{ Removal} = \frac{(C_0 - C_t)}{C_0} \times 100 \quad (3.8)$$

### 3.11 OPTIMIZATION OF OPERATIONAL VARIABLES

In this section, effect of various parameters or operational variable such as effect of adsorbent dose, Contact time, pH, initial concentration and temperature on the adsorption of RhB dye by AMC and ANC have been examined. Kinetics studies for the removal of the dye under the given condition have also been to understand the mechanistic role of the system. The experiments were repeated twice and suitable resulted value was reported.

#### i) EFFECT OF ADSORBENT DOSE

The effect of adsorbent (AMC and ANC) dose on the RhB adsorption was investigated by the varying the amount of dose from 0.2g to 3.2g (with 0.2 difference in dose quantity) in 50ml dye solution. These experiments were carried out at natural pH using 100mg/L or 100 ppm of initial dye concentration for exactly 360 minutes. The minimum amount of adsorbent corresponding to the cross section of uptake capacity and percentage removals.

#### ii) EFFECT OF CONTACT TIME

The effect of contact time on the adsorption of RhB dye on to AMC and ANC were studies in the range of 0 to 360 minutes (as 15,30,45,60,120,180,240,300 and 360 minutes). This study was carried out at natural pH of all dye solution using 50 ml of 100 mg/L of initial adsorbate concentration and 10 g/L of AMC and 24g/L of ANC. As the time of agitation increases, the intimate contact between sorbate-sorbent increased and all the pores of adsorbent was occupied by the adsorbate in monolayer fashion initial stages.

#### iii) EFFECT OF PH

Effect of pH on the adsorption of RhB dye by AMC and ANC was studies in the pH range 2.0 to 12.0. The pH of RhB solution were adjusted prior to the experiments using the 0.1M NaOH and 0.1M HCl. The pH values of the solution were measures before and after the sorption process and change in pH was examined. This study was conducted with 50 ml of 100 mg/L initial adsorbate concentration and 10 g/L of AMC and 24g/L of ANC.

#### iv) EFFECT OF INITIAL CONCENTRATION

The effect of initial adsorbate concentration ( $C_0$ ) on the adsorption by AMC and ANC was examined by ranging the initial concentration from 50-150 mg/L of 50 ml. This study

conducted at pH 4 with adsorbent dose 10 g/L for AMC and pH 12 with adsorbent dose 24g/L for ANC. Time of agitation for this experiment was 360 minutes. The rate limiting step in the reaction is defined as the adsorption which is concentration dependent .When the kinetics of the reaction is controlled by intra particle transport, Variation in the reaction rate is not expected to be linear, whereas the rates of the strictly adsorptive reaction and simple diffusion controlled process are expected to be proportional to the first power of the adsorbate concentration.

#### v) EFFECT OF TEMPERATURE

Here investigation was done and the influence of temperature on the sorption rates was examined at four different temperatures (35 °C, 45 °C, 55 °C and 65 °C). The Effect of the temperature for the adsorption of RhB dye was studied at pH 4 for AMC with 10g/L adsorbent dosage and pH 12 for ANC with 24g/L adsorbent dosage for 360 minutes with 50 ml dye solution having six different concentration (30,50,100,150,200 and 250 mg/L). From this temperature effect, different isotherms studies were also did for choosing of better fitting isotherm.

### 3.12 THERMODYNAMIC PARAMETERS

Since the adsorption is a kinetic process, removal rate can be increased or decreased by increase or decrease in the system temperature. The Gibbs free energy change ( $\Delta G^0$ ) of the sorption process is related to the equilibrium constant by the classic Van't Hoff equation

$$\Delta G^0 = -RT \ln K_d \quad (3.9)$$

According to thermodynamics, the Gibbs free energy change is also related to the entropy change and heat of adsorption at constant temperature by the following equation:

$$\Delta G^0 = \Delta H^0 - T\Delta S^0 \quad (3.10)$$

Combining equations 3.9 and 3.10, we get

$$R \ln K_d = \frac{-\Delta G^0}{T} = \Delta S^0 - \frac{\Delta H^0}{T} \quad (3.11)$$

Where,  $K_d$  is the distribution coefficient,  $\Delta H^0$  is the enthalpy change (kJ/mol),  $\Delta S^0$  is the entropy change (J/K mol), R is the gas constant (8.314 J/K.mol) and T is the temperature in kelvin.

If the process is endothermic ( $\Delta H^0 > 0$ ), the equilibrium constant increases with temperature, if the process is exothermic ( $\Delta H^0 < 0$ ), the equilibrium constant decreases as temperature is raised. Gibbs free energy of the specific sorption was calculated from the well-known equation (3.9). The thermodynamic parameters  $\Delta H^0$  and  $\Delta S^0$  were obtained from the slope and intercept of the linear Van't Hoff plot ( $R \ln K_d$  vs.  $1/T$ ).

### 3.13 MODELING OF ADSORPTION ISOTHERMS AND ITS STUDIES

To determine the efficiency of the sorbents prepared, the equilibrium sorption of the RhB dye was studied as a function of concentration. Several equilibrium models have been developed to describe sorption isotherm relationships. Any particular may be fit experimental data accurately in one set of conditions, but may be fall entirely under another. No single model has been found to be applicable in generals. The sorption of capacities of Activated Mahua seed carbon (AMC), activated Bael Shell carbon (AAM), Activated Neem seed Carbon (ANC) and activated abrus Precatorius Carbon (APC) for Rhodamine B have been evaluated using different isotherms, namely Langmuir, Freundlich, Temkin and Dubinin-Raushkevich (D-R) isotherms.

#### 3.13.1 Langmuir Isotherm

The most widely used isotherm equation for modeling of the adsorption data is the Langmuir equation, which is valid for monolayer sorption onto a surface with a finite number identical site and is given by following equation.

$$q_e = \frac{a_L b_L C_e}{1 + b_L C_e} \quad (3.12)$$

Generally in Langmuir theory the basic assumption is that the sorption takes place at the specific homogeneous sites with in with in the sorbent. The basic assumptions underlying the Langmuir model, which is also called the ideal localized monolayer models are:

- a) Solute molecules are adsorbed on definite site on the sorbent surface,
- b) Each site can accommodate only one molecules,
- c) The area of each site is a fixed quantity determined solely by the geometry of surface,
- d) The sorption energy is the same at all sites,
- e) The adsorbed molecules cannot migrate across the surface or interact with the neighboring molecules and, f) Adsorption may be reversible

For solid liquid systems, the Langmuir isotherm is expressed in the linear form as:

$$\frac{C_e}{q_e} = \frac{1}{Q_{\max} b_L} + \frac{C_e}{Q_{\max}} \quad (3.13)$$

Where,

$Q_{\max}$  = monolayer adsorption capacity, (mg.g<sup>-1</sup>), signifies the solid phase concentration, corresponding to the complete coverage of available sorption site, can be evaluated from the slope of Langmuir isotherm plot ( $C_e/q_e$  against  $C_e$ )

$b_L$  = Langmuir Isotherm constant, (L.g<sup>-1</sup>) ,This value corresponds to energy of sorption, calculated from the intercept of the linear plot of Langmuir isotherm.

The influence of the isotherm shape for ‘favorable’ and ‘unfavorable’ sorption, on the basis of feasibility criteria, was studied by Weber and Chakraborti .The essential characteristics of Langmuir isotherm can be expressed in terms of a dimensionless separation factor , $R_L$  ,which describe the type of isotherms and is defined by,

$$R_L = \frac{1}{1 + b.C_0} \quad (3.14)$$

Where,  $b$  is Langmuir constant introduced in equation (3.13) and  $C_0$  is the initial concentration. The parameters indicate the shape of the isotherm accordingly, if,  $R_L$  value lies in between 1 to 0, then favourable adsorption indicated. If,  $R_L$  value greater than 1, unfavourable adsorption, while a value of 1 represents linear & unfavourable and 0 represents irreversible.

### 3.10.2 Freundlich Isotherm

The freundlich isotherm model is derived by assuming a heterogeneous surface with a non-uniform distribution of heat of adsorption over the surface, the freundlich model is non-linear & linear form can be expressed as

$$q_e = K_F (C_e)^{1/n} \quad (3.15)$$

$$\ln q_e = \ln K_F + \frac{1}{n} \ln C_e \quad (3.16)$$

Where,  $K_F$  is the freundlich characteristics constants and  $1/n$  the heterogeneity factor of adsorption, obtained from intercept and slope of  $\ln(q_e)$  vs  $\ln(C_e)$  linear plot respectively.



The value of  $K_f$  is an indicator of adsorption capacity and thus can be used for relative measurement of the surface area.  $b$  and  $1/n$  are related to enthalpy and intensity of the adsorption.  $1/n$  value should be less than unity for high adsorption capacity.

### 3.13.3 Temkin Isotherm

The temkin equation isotherm assume that the heat of adsorption of all the molecule in the layer decreased linearly with coverage due to sorbent-sorbate interaction and that adsorption is characterised by uniform distribution of the binding energy, up to some maximum binding energy . The value of temkin constant along with the coefficient of determination. The temkin isotherm can be expressed as

$$q_e = \frac{RT}{b \cdot \ln(K_T C_e)} \quad (3.17)$$

Equation 3.17 can be linearized as:

$$q_e = B_1 \ln K_T + B_1 \ln C_e \quad (3.18)$$

Where ( $B_1=RT/b$ ) and  $K_T$  is the equilibrium binding constant (L/mg) corresponding to the maximum binding energy and the constant  $B_1$  is related to the heat of sorption. A plot of  $q_e$  versus  $\ln(C_e)$  enables the determination of the isotherm constant  $K_T$  and  $B_1$ .

### 3.13.4 Dubinin-Radushkevich (D-R) Isotherms

The dubinin-radushkevich (D-R) isotherm model for pore filing nature of the sorption process can be given as: in Ahmaruzzaman et.al.[29]

$$\ln q_e = \ln X_m - \beta \varepsilon^2 \quad (3.19)$$

Where  $q_e$  is the amount of sorbate-sorbed onto sorbent and  $X_m$  (mg/g) represents the maximum sorption capacity of sorbent,  $\beta$  is constant related to sorption energy, while  $\varepsilon$  is Polanyi sorption potential ,which can be obtained by following equation:

$$\varepsilon = RT \ln \left( 1 + \frac{1}{C_e} \right) \quad (3.20)$$

Where  $R$  is gas constant in kJ/mol K,  $T$  is temperature in kelvin and  $C_e$  is the equilibrium concentration of adsorbate in solution.

When  $\ln(q_e)$  is plotted against  $\epsilon^2$ , a straight line is obtained. The slope of the plot gives the value of B and the intercept yields the value of sorption capacity  $X_m$ . The constant  $\beta$  gives the mean free energy 'E' of sorption per molecules of sorbate when it is transferred to the surface of the solid from infinity in the solution and can be computed using the following relationship.

$$E = \frac{1}{\sqrt{-2\beta}} \quad (3.21)$$

The value of E gives information whether the sorption mechanism is ion-exchange, chemical or physical sorption.

### 3.14 ADSORPTION DYNAMICS

The kinetic of sorption is important from the point of view that it controls the process efficiency. The characterization of sorbent surface is a critical factor that affects the rate parameters and that diffusion resistance plays an important role in the overall transport of the solute. The kinetics of sorption that define the efficiency of sorption of Rhodamine B dye were checked by the pseudo first order, pseudo second order models.

#### 3.14.1 Pseudo First Order Model

The first order rate expression given by langergren:

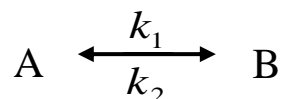
$$\log(q_e - q) = \log q_e - k_{ad} \left( \frac{t}{2.303} \right) \quad (3.22)$$

Where,  $q_e$  and  $q$  are the amount of dye adsorbed (mg/g) at time  $t$  (min) and at equilibrium time, respectively and  $k_{ad}$  is the rate constant of the adsorption [30~32,34,36,37].

For controlling of kinetics four steps were present, (a) mass transfer of solute from solution to the boundary film, (b) mass transfer metal ions from boundary film to surface, (3) sorption and ion exchange of ions onto site, (4) internal diffusion of solute. This step is assumed to be very rapid and non-limiting in this kinetic analysis: sorption is a rapid phenomenon. The first and the second steps are external mass transfer resistance steps, depending on various parameters such as agitation and homogeneity of solution. The fourth one was particle diffusion resistance step.

Using the kinetic equations, the overall rate constant, the forward and backward rate constants were calculated at variable parameter concentration and temperature. The sorption of chromium from liquid to solid phase may be expressed as

Here forward reaction constant is  $K_1$ , and Backward reaction constant  $K_2$ .



Where,  $K_1$  is the forward reaction rate constant,  $k$  the backward reaction rate constant. Using the kinetic equations in our early publication overall rate constant, the forward and backward rate constants were calculated at different temperature. By plotting  $\ln(1-Ut)$  versus  $t$ , the overall rate constant  $k$  for given concentration of Rhodamine B was calculated by considering the slope of straight line in Fig. for various temperature and concentration (Rengaraj et al.[30]). By using equations in reference, the equilibrium constant  $K_c$ , forward and backward rate constants  $k_1$  and  $k_2$  were calculated and shown in Table . From this table, it is seen that the forward rate constants for the removal of B dye higher than the backward rate constants namely the desorption process. This result shows that the rate of adsorption is clearly dominant.

### 3.14.2 Pseudo Second Order Model

The pseudo 2<sup>nd</sup> order model can be represent in the following form, Ahmaruzzaman et.al.[29]

$$\frac{dq_t}{dt} = K_2(q_e - q_t)^2 \quad (3.23)$$

Where,  $K_2$  is pseudo second order rate constant (g/mg .min)

After integrating the equation (3.19) for boundary conditions  $q_t=0$  at  $t=0$  and  $q_t=q_t$  at  $t=t$ , the following equation is obtained

$$\frac{t}{q_t} = \frac{1}{(K_2 q_e^2)} + \frac{1}{q_e} t \quad (3.24)$$

The initial Sorption rate,  $h$  (mg/g.min), at  $t \rightarrow 0$  is defined as:

$$h = K_2 \cdot q_e^2 \quad (3.25)$$

The initial sorption rate  $h$  (mg/g.min), the equilibrium sorption capacity ( $q_e$ ), the pseudo second order constant  $K_s$  can be calculated from the slope and intercept of plot  $t/q_t$  vs.  $t$ .

## Result and Discussion

In this section, different experiments were done and these experimental results were very nicely discussed on the basis of scientific occurrence.

### 4.1 Calibration Curve

A calibration is a general method of determining the concentration of a substance in a unknown sample by comparing it with the known concentration having a set of standard sample. It knows as analytic signal as because of the calibration curve plotted according to the instrumental response and it changes with concentration of the measured substance (analyte). The operator prepares a series of standards across a range of concentrations near the expected concentration of analyte in the unknown. The concentrations of the standards must lie within the working range of the instrumentation. For most analyses a plot of instrument response vs. analyte concentration will show a linear relationship. The operator can measure the response of the unknown and, using the calibration curve, can interpolate to find the concentration of analyte or the unknown concentration.

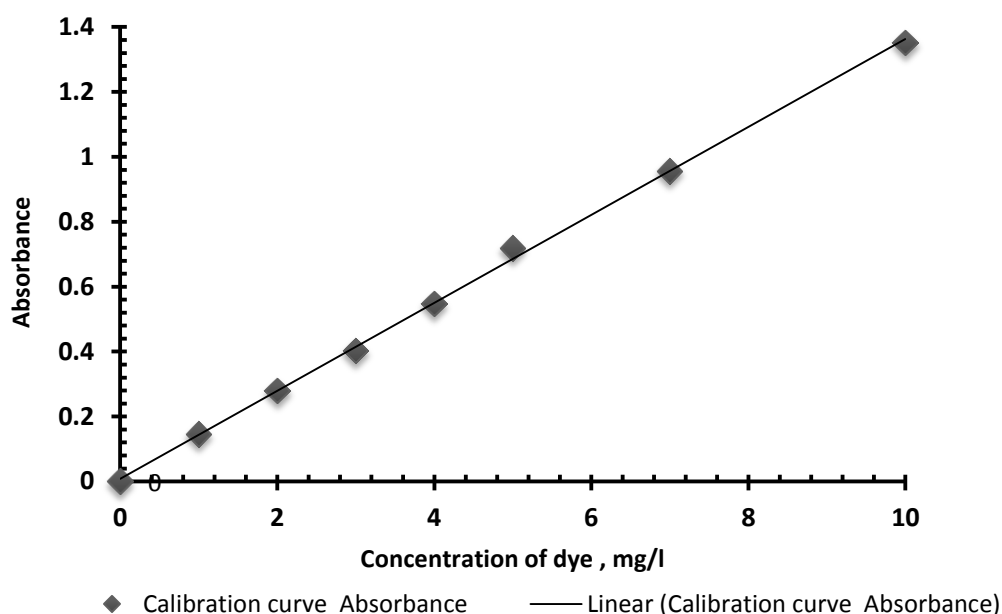


**Figure 4.1:** Graphical representation of calibrating of unknown RHB dye concentration in the water sample,  $C_0 = 0$  mg/l to 20 mg/l,  $T = 25^\circ\text{C}$

In the calibration curve method, a series of external standard solutions is prepared and measured. A line or curve is fit to the data and the resulting equation is used to convert

readings of the unknown samples into concentration. An advantage of this method is that the random errors in preparing and reading the standard solutions were averaged over several standards. Moreover, non-linearity in the calibration curve can be detected and avoided (by diluting into the linear range) or compensated (by using non-linear curve fitting methods).

Most analytical instruments generate an electrical output signal such as a current or a voltage. A calibration curve establishes the relationship between the signal generated by a measurement instrument and the concentration of the substance being measured. Different types of chemical compounds and elements give different signals. When an unknown sample is measured, the signal from the unknown is converted into concentration using the calibration curve.

Preparation of a series of "standard solutions" of the substance that you intend to measure, measure the signal (e.g. absorbance, if you are doing absorption spectrophotometry), and plot the concentration on the x-axis and the measured signal for each standard on the y-axis. Drawing a straight line as close as possible to the points on the calibration curve (or a smooth curve if a straight line won't fit), so that as many points as possible were right on or close to the curve.

## **4.2 Various parametric effects on the adsorption of Rhodamine B (RhB) dye onto Activated Mahua carbon (AMC):**

### ***4.2.1 Effect of adsorbent (AMC) Dosage on adsorption***

In adsorption studies the adsorbent dose play a important role, because of effective removal of adsorbent and cost of used adsorbent .Using of less adsorbent dose then the required achievable removal or using more costlier adsorbent dose for getting optimum removal, so to answer these drawbacks, choosing of intermediate path is always cost effective path for maximum removal with minimal resources. So there is huge importance for the study of effect of adsorbent doses on adsorption for all adsorption studies [30, 33, 37].

In order to study the effect of adsorbent dosages, different dosages of AMC (Activated Mahua seed carbon) were taken as varies from 0.2 g to 2.2 g into series of 100 ml conical flasks which contain 50 ml of RhB dye of 100 ppm (100 mg/l) concentration. The sample is kept in shaker for 6 hours with nearly 120 rpm for better mixing at solid liquid interface. Here natural pH was maintained. A plot of  $Q_e$  and % removal was plotted on same axis against the adsorbent dosage.

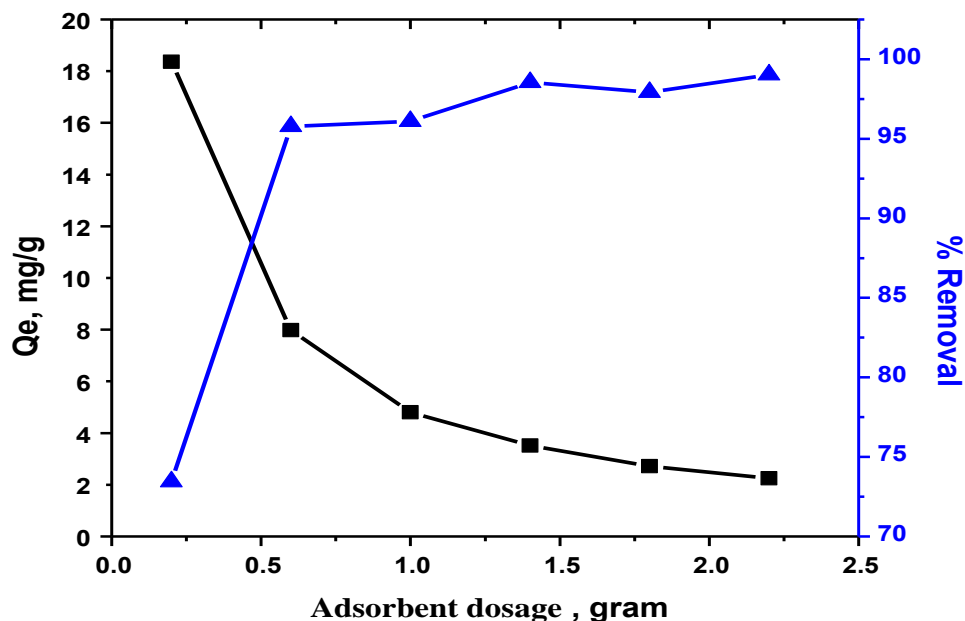


**Figure 4.2:** Graphical presentation of adsorbent dosage effect on adsorption process,  $V=50$  ml,  $C_0=100$  mg/g, adsorbent dosage = 0.2g to 2.2g, Stirring period = 360 minutes,  $T = 25^\circ\text{C}$ , Natural pH & at aerobic condition

It was found in the Fig.4.2, that with increase in AMC adsorbent dose percentage removal is increased because large amount of adsorption sites were found, in contrast the uptake of RhB dye is gradually decreased because of two reasons, firstly for the same amount of RhB dye large number of adsorption sites were found and secondly large amount of adsorbents in the small available space clump together thereby limiting the path of diffusion and thus adsorption. The corresponding point on x-axis of the intersection point of these two curves give the optimal dose of adsorbent and here we found the optimal dose for AMC as 0.5g/ 50 ml (10 g/l) of RhB dye solution

#### 4.2.2 Effect of Contact Time on RhB-AMC system

To investigate the effect of contact time on adsorption of RhB dye ( $C_0=100$  mg/L), the batch experiments were carried out in a series of conical flasks with a constant AMC dose of 0.5gm/50 ml in all the samples as optimal dose. These flasks were agitated in water bath shaker for 15, 30, 45, 60, 120, 180, 240, 300 and 360 minutes at a constant 120 rpm at the natural pH in all the samples. The samples were withdrawn from the water bath shaker at predetermined time intervals. The settled supernatants were bring out from flask using prepette after giving sufficient time and subsequently with syringe driven whatman Millipore filter of pore size  $0.45\mu\text{m}$ . The concentration of dye in supernatant was measured for all the samples. The  $Q_e$  was evaluated for all the samples and a graph was plotted between  $Q_e$  vs time.

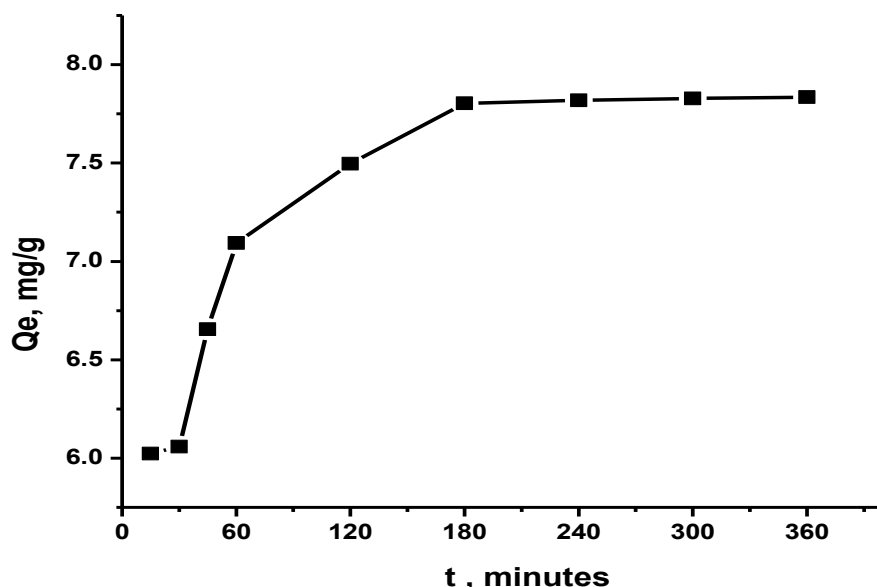


**Figure 4.3:** Graphical representation of contact time effect on adsorption process,  $V=50$  ml,  $C_0=100$  mg/g, Adsorbent dose =  $0.5\text{g}/50$  ml dye solution, Stirring period =15 to 360 minutes, natural pH,  $T = 25^\circ\text{C}$

From this above graph, we explained that nearly after 180 minutes  $Q_e$  equilibrium reached and % Removal also became constant, so the optimal contact time was 180 minutes. This optimal time period was the sufficient time for stabilization of this adsorbent and adsorbate dispersed solution.

#### 4.2.3 Effect of pH on RhB-AMC system

One of the most important parameters controlling the adsorption process is pH. The effect of pH of the solution on the adsorption of RhB on AMC was determined. The pH of the solution was controlled by the addition of 0.1M HCl or 0.1M NaOH. The uptake of RhB at pH 11.0-12.0 was the minimum and a maximum uptake was obtained at pH 4.0. However, when the pH of the solution was increased (more than pH 3), the uptake of RhB was increased. It appears that a change in pH of the solution results in the formation of different ionic species, and different carbon surface charge. At pH values lower than 6, the dye can enter into the pore structure. At a pH value higher than 6, the zwitterions form of RhB in water may increase the aggregation of RHB to form a bigger molecular form (dimer) and become unable to enter into the pore structure of the carbon surface.

At a pH value higher than 10, the existence of  $\text{OH}^-$  creates a competition between  $-\text{N}^+$  &  $\text{COO}^-$  and it will decrease the aggregation of RhB, which causes an increase in the adsorption of dye on the carbon surface. Due to the amphoteric character of a carbon surface, its adsorption properties may be influenced by the pH value of the solution.

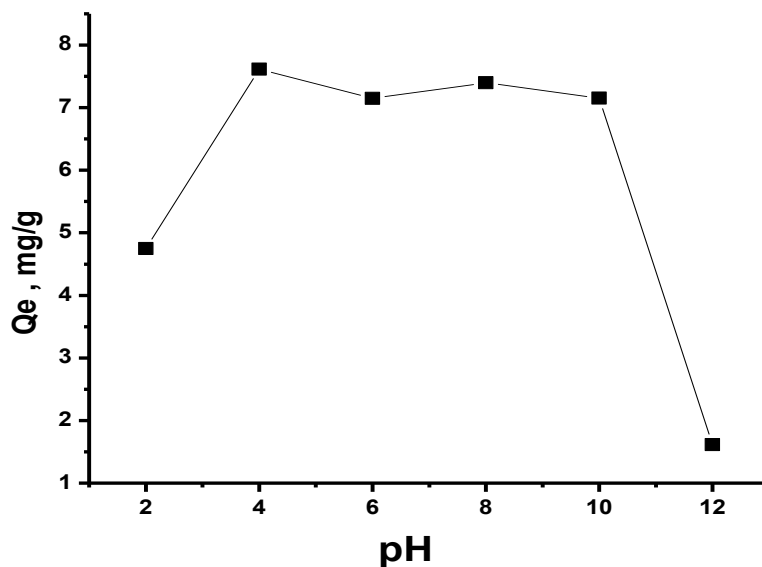


**Figure 4.4:** Graph of pH effect on adsorption process,  $V=50$  ml,  $C_0=100$  mg/g, Adsorbent dosage =0.5 g/50 ml of dye solution, Stirring period =180 minutes, pH = 2 to 12 (maintained).  $T = 25^\circ\text{C}$

The effect of initial pH on the adsorption of dye was also evaluated at  $25^\circ\text{C}$  at different initial pH values in the range of 2–12 for initial concentrations of 100 mg/l for RhB dye solution adjusted by adding either 0.1M HCl or 0.1M NaOH.

#### 4.2.4 Point Zero Charge for RhB-AMC system

The pH at the potential of zero charge of the carbon ( $\text{pH}_{\text{zpc}}$ ) was measured using the pH drift method. pH taken as 1.05,2,3,4,5,6,7,8,9,10,11,12 and 12.93.

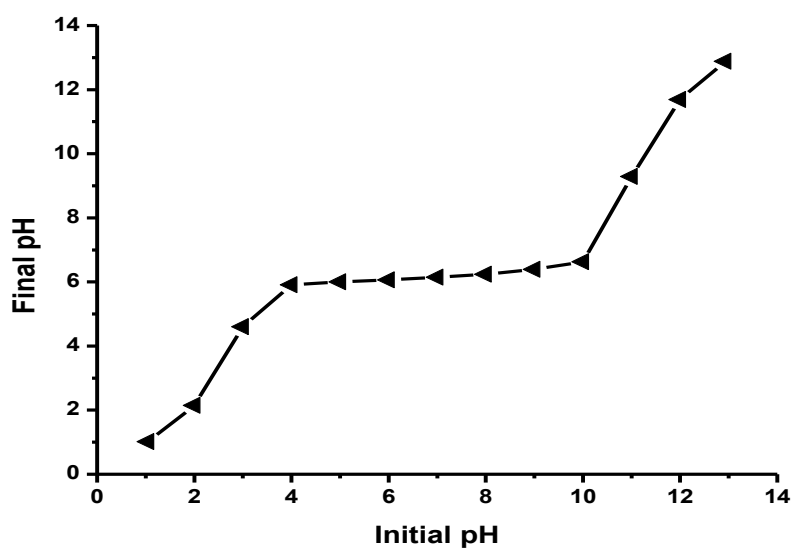


**Figure 4.5:** Graph of pH effect on adsorption process,  $V=50$  ml,  $C_0=100$  mg/g, Adsorbent Dosage = 1 g/50 ml of dye solution, Stirring time =180 minutes, pH = 2 to 13 (maintained),  $T = 25^\circ\text{C}$



The pH of the solution was adjusted by using 0.1 M sodium hydroxide or hydrochloric acid. 1 g of the activated carbon was added to 50 ml of 100 ppm solution. After stabilization, the final pH was recorded. The plot of final pH versus initial pH was used to determine the zero point charge of the activated carbon [38, 40].

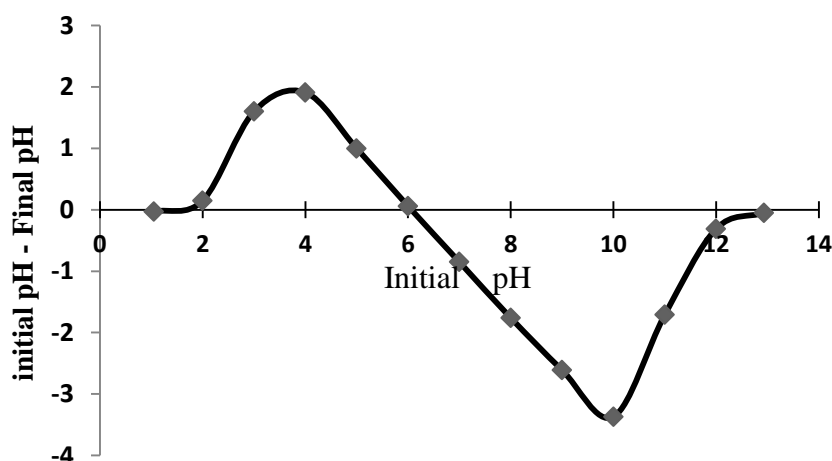


**Figure 4.6:** Graphical representation of initial pH vs (initial pH– final pH)

Therefore, It can be assumed that  $pH_{zpc}$  of RhB dye-AMC system is pH 6.0. Then surface of the activated carbon AMC is negatively charged above the  $pH_{zpc}$ , and positively charged below the  $pH_{zpc}$ . The magnitude of surface charge of activated carbon decreases with increase in pH. Thus, electronegativity of activated increases with increase in pH. The lower removal of the positively charged dye at acidic pH range is probably due to the presence of excess  $H^+$  ions was competing with the dye molecule for the adsorption site. At alkaline pH, adsorbent surface gets net negative charge.

Therefore, there is an attractive electrostatic force between  $pH_{zpc}$  molecule (positively charged dye molecules) and adsorbent. The decrease in removal of RhB with increase in pH above pH 10 can be attributed to the presence of an acidic group. The acidic group (carboxylic group) may dissociate as the pH increases, giving rise to a net negative charge on dye molecule.

#### **4.2.5 Effect of initial Concentration of RhB-AMC system**

To study the effect of initial dye concentration, experiments were carried out in different conical flasks with a fixed adsorbent dose of 0.5g/50ml at varying RhB dye concentrations of 50,100 and 150  $mg.L^{-1}$ . All the solution maintained the pH as 4.0. Each particular dye concentration shaking for 15,30,45,60,120,180,240,300,360 minutes.

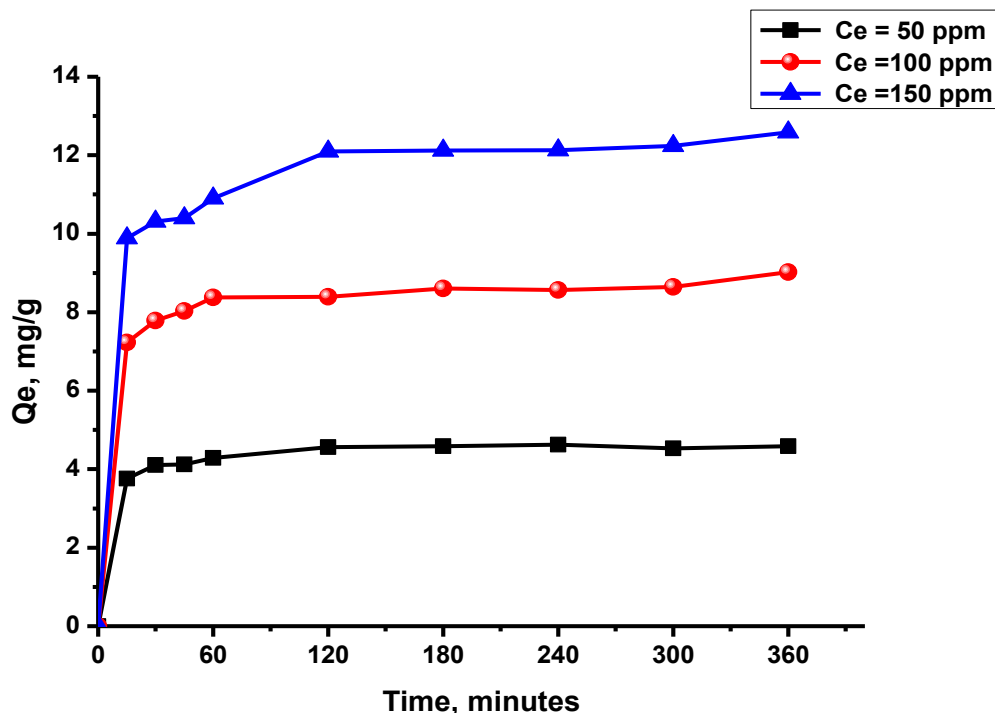


**Figure 4.7:** Graphical representation of initial concentration effect on adsorption process,  $V=50$  ml,  $C_0=100$  mg/g, Dosage =  $0.5$  g/50 ml of dye solution, Stirring time = 180 minutes,  $pH = 4.0$  (maintained),  $T = 25^\circ C$

The samples were withdrawn from the shaker at the mentioned time intervals. Post adsorption the supernatant was collected and filtered, first using then by syringe driven  $0.45\mu m$  Millipore whatman filter. Filtered supernatant was analyzed using spectrophotometer and a graph was plotted with  $Q_e$  versus time. The adsorption data for the uptake of phenol versus contact time at different initial concentrations is represented in Fig.4.7 below.

From the Fig.4.7, here the pattern of graph showing that nearly 92% removal of dye with an initial concentration of 50 ppm and the equilibrium is reached 180 mins. However with initial concentration of 100 ppm about 90% removal is becoming possible and equilibrium was in the approaching state at the end of 180 mins and the results with the initial concentration of 150 ppm have shown 83% of dye removed and equilibrium achieved at 120 mins equilibrium. 50% of the total amount of dye uptake was found to occur in the first 15 minutes and the adsorption process was almost tending towards equilibrium at the end of 360 minutes. The higher sorption rate at initially may be due to an increased in concentration gradients between adsorbate in solution and adsorbate on adsorbent surface, as time precedes this concentration gradient is reduced due to the accumulation of dye particles in the vacant sites leading to a decrease in the sorption rate at the larger stages from 15 to 360 minutes.

## 4.2.6 KINETIC OF ADSORPTION

Generally for kinetics of adsorption study pseudo-first-order and pseudo-second order models were considered. The different results were collected from these graphs. The contact time study can be used to determine the rate limiting step in the adsorption process with the help of a Weber –Morris plot. The possible rate limiting steps were mass transfer from the bulk liquid phase to the particle external surface, film diffusion and inter particle diffusion.

### Kinetic of adsorption of AMC and RHB dye system

The time dependent batch adsorption data using fixed dose 0.5 gm with pH = 4 maintained of adsorbent at 25 °C was used for kinetic modeling of the different dye system with an initial concentration of 1000 mgL<sup>-1</sup>

#### 4.2.6.1 Pseudo first order kinetic model

The linearized form of pseudo-first-order kinetics is given by equation (3.22) in chapter 3 it is clear that, in figure 4.8 a plot of  $\ln(1-Ut)$  Vs.  $t$  (time) should give a linear relationship with the slop  $K_1$  and intercept of  $\ln(Q_e)$ .

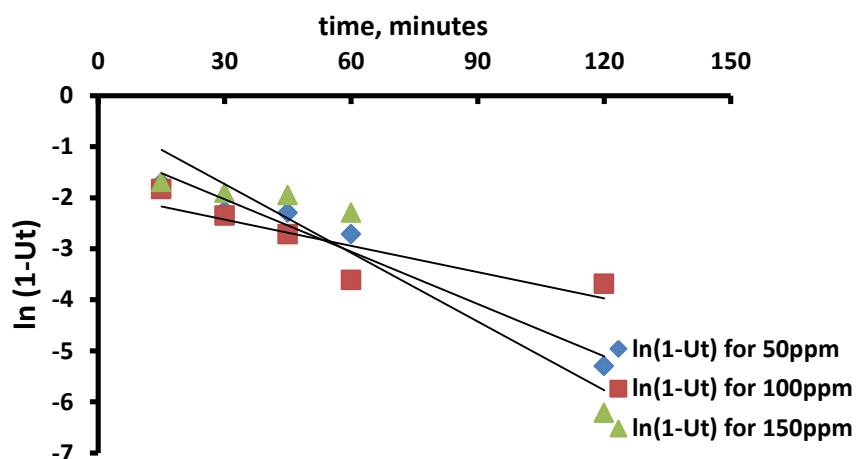


**Figure 4.8:** Pseudo first order kinetic model for AMC –RhB system; Adsorbent Dose =0.5g/50 ml of dye solution,  $C_0$ = 50,100 and 150 mg/g, pH = 4.0, T = 25 °C

**Table 4.1 :**Pseudo-first-order kinetic constants for the adsorption

$C_0$ (mg/L)	Kc	overall rate constant $K = K_1 + K_2$ (h <sup>-1</sup> )	Forward rate constant $K_1$ (h <sup>-1</sup> )	Backward rate constant $K_2$ (h <sup>-1</sup> )	$R^2$
50	11.077	0.025	0.02293	0.00207	0.962
100	6.152	0.0173	0.014881	0.002419	0.749
150	4.208	0.0468	0.037813	0.008987	0.901

#### 4. 2.6.2 Pseudo Second order kinetic model

The linearized form of pseudo-second-order kinetics is given by equation (3.24) in chapter 3. In figure 4.9 a plot of  $t(\text{time})$  Vs.  $t/Q_t$  should give a linear relationship with the slope  $1/q_t$  and with intercept of  $1/(K_2(q_t)^2)$

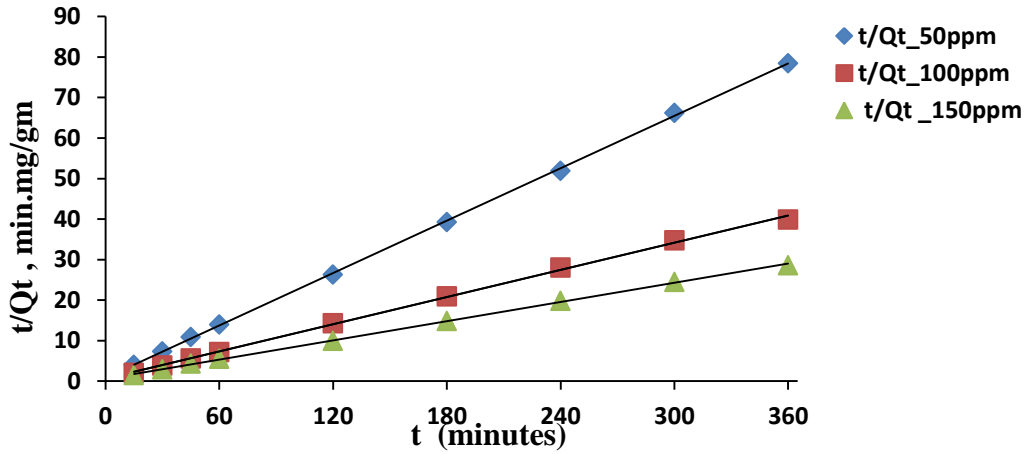


**Figure 4.9:** Pseudo second order kinetic model for AMC –RhB system; Dose =0.5g/50 ml of dye solution,  $C_0= 50,100$  and  $150 \text{ mg/g}$ , pH = 4.0 (maintained),  $T = 25^\circ\text{C}$

50	4.638	0.5703	0.9998
100	8.953	0.0173	0.9989
150	12.69	0.0101	0.9994

#### 4.2.7 Effect of Temperature

Here the effect of temperature was studied with different temperatures such as  $35^\circ\text{C}$ ,  $45^\circ\text{C}$ ,  $55^\circ\text{C}$  and  $65^\circ\text{C}$ . Here experiments were performed at adsorbent dose = 0.5g/50 ml of dye solution, pH = 4 and agitation period 180 minutes with 120 rpm [29, 38].

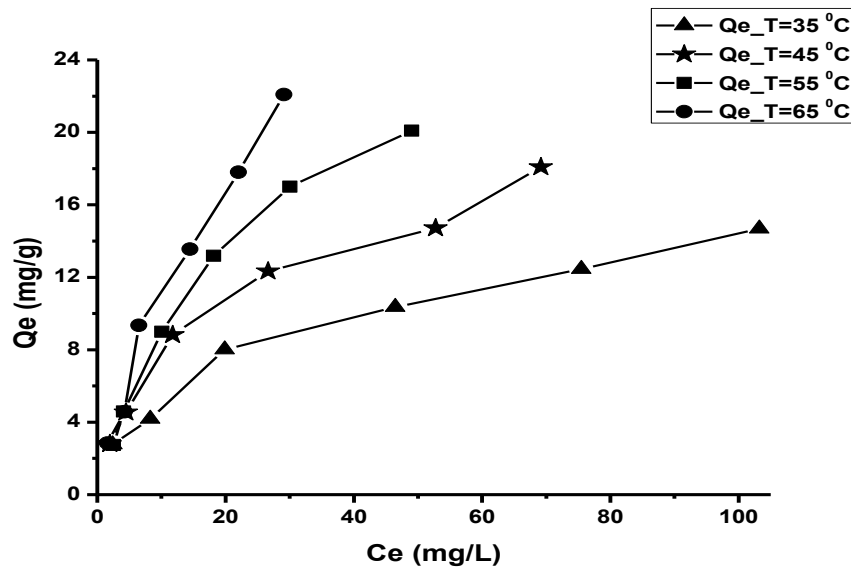


**Figure 4.10:** Adsorption equilibrium of different temperature for RhB –AMC system

The temperature studies show that optimum adsorption takes place at 65<sup>0</sup> C. In fig.4.9, the adsorption capacity of dye increased at higher temperature, which clearly indicates that adsorption of dye in this system, was an endothermic process. For higher temperature the surface coverage increased, may be because of increase of dye penetration inside micro pores at higher temperatures or the creation of new active site as increase surface area. From fig.4.9, it was visualized that adsorption capacity increases with temperature 35<sup>0</sup>C < 45<sup>0</sup>C < 55<sup>0</sup>C < 65<sup>0</sup>C.

#### 4.2.8 Adsorption equilibrium study

Equilibrium study on adsorption provides information on the capacity of the adsorbent. An adsorption isotherm is characterized by certain constant values, which express the surface properties and affinity of the adsorbent and can also be used to compare the adsorptive capacities of the adsorbent for different pollutants. For this equilibrium study of our work, we have considered four basic isotherm models namely Langmuir, Freundlich, Temkin and D-R isotherm models [29-33, 37].

##### Adsorption equilibrium study for RhB - AMC system

###### i) Langmuir isotherm

The linearized form of Langmuir isotherm is given by equation 3.13 of chapter-3. The Langmuir constant  $Q_0$ ,  $a_L$  and  $b_L$  can be calculated by plotting  $C_t/Q_e$  vs.  $C_t$ .

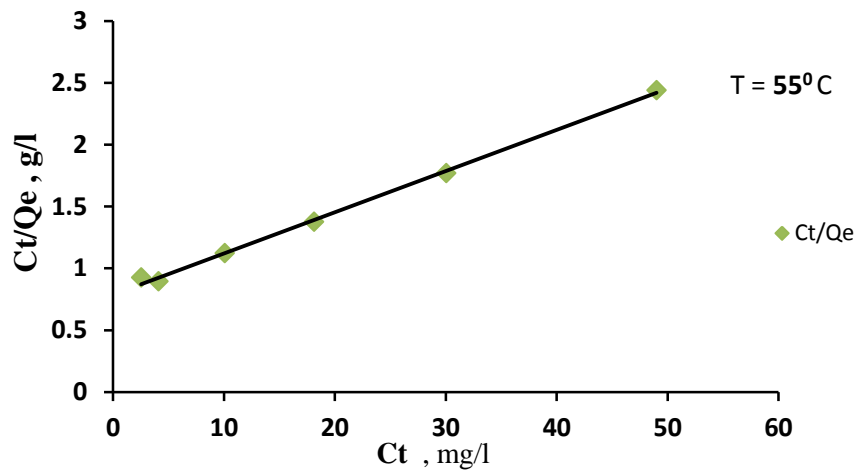


**Figure 4.11:** Langmuir isotherm for RhB- AMC system

Similarly In the similar way Langmuir isotherm plots for RhB-AMC adsorption system at other temperatures were also made and the various parameters calculated from those plots were tabulated below.

**Table 4.3:** Langmuir isotherm parameters

Temp(°C)	$Q_{max}$ (mg/g)	$b_0$ (mg/g)	$R^2$
35	16.722	0.047	0.974
45	20.833	0.063	0.979
55	30.303	0.042	0.997
65	39.683	0.039	0.848

## ii) Freundlich isotherm

The linearized form of Freundlich isotherm for RhB-AMC system, is given by equation 3.16 of chapter-3. The value of  $K_F$  and  $n$  can be calculated by plotting  $\ln(Q_e)$  versus  $\ln(C_e)$ .

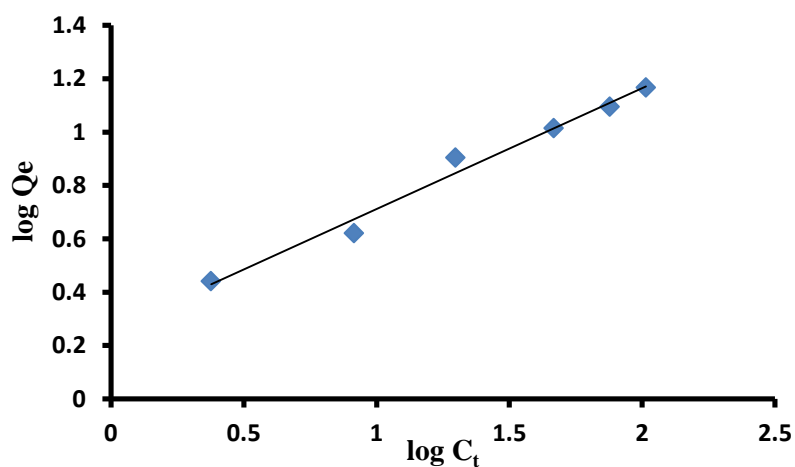


Figure 4.12: Freundlich isotherm for RhB- AMC system

In the similar way Freundlich isotherm plots for adsorption systems at other temperatures were also made and the various parameters calculated from those plots were tabulated below.

Table 4.4: Freundlich isotherm parameters

Temp( $^{\circ}$ C)	n	$K_F$	$R^2$
35	2.211	1.296	0.984
45	1.954	1.391	0.982
55	1.485	1.256	0.978
65	1.388	1.343	0.973

## (iii) Temkin Isotherm

The linearized form of Temkin isotherm is given by equation 3.18 of chapter-3. The value of  $K_T$  and  $B$  can be calculated by plotting  $Q_e$  Vs.  $C_t$ .

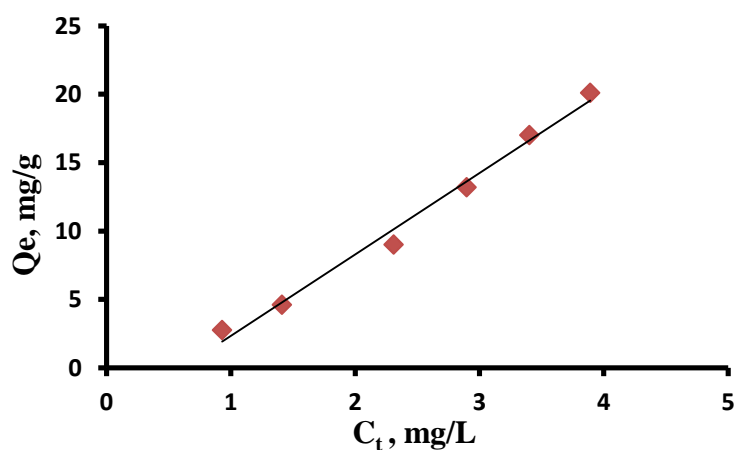


Figure 4.13: Temkin isotherm for RHB- AMC system

In the similar way Temkin isotherm plots for RHB dye -AMC adsorption systems at other temperatures were also made and the various parameters calculated from those plots were tabulated below.

**Table 4.5:** Temkin isotherm parameters

Temp(°C)	B	K <sub>T</sub>	R <sup>2</sup>
35	3.161	0.696	0.954
45	4.167	0.790	0.975
55	5.985	0.543	0.988
65	6.608	0.682	0.932

**(iv) D-R isotherm**

The linearized form of D-R isotherm is given by equation 3.19 of chapter-3. The value of  $\emptyset_D$  and  $\psi_D$  can be calculated by plotting  $Q_e$  vs.  $C_t$ .

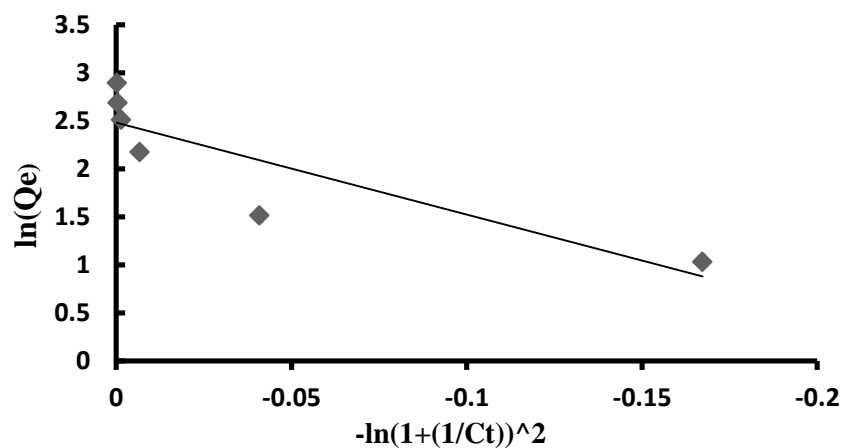


**Fig 4.14:** D-R isotherm for RHB- AMC system

In the similar way D-R isotherm plots for RHB dye AMC adsorption systems at other temperatures were also made and the various parameters calculated from those plots were tabulated below.

**Table 4.6:** D-R isotherms Parameters

Temp(°C)	$\emptyset_D$	$\Psi_D$	R <sup>2</sup>
35	2.669	3.37	0.646
45	4.032	3.535	0.988
55	3.179	4.567	0.866
65	3.099	4.046	0.696

### 4.3 Various parametric effects on the adsorption of Rhodamine B (RhB) dye onto Activated Neem carbon (ANC):

As like previously done in case of RhB –AMC ,same techniques were followed for different operational variable or parameter studies of adsorption ,only new is that activated neem carbon(ANC) took as adsorbent for RhB-ANC adsorption system.

#### 4.3.1 Effect of adsorbent dosage on RhB-ANC system

In order to study the effect of adsorbent dosages, different dosages of ANC (Activated Neem seed carbon) were taken as varies from 0.2 g to 3.2 g into series of 100 ml conical flasks which contain 50 ml of RhB dye of 100 ppm (100 mg/l) concentration. The sample is kept in shaker for 6 hours with nearly 120 rpm for better mixing at solid liquid interface. Here natural pH was maintained. A plot of  $Q_e$  and % removal was plotted on same axis against the adsorbent dosage [30, 33].

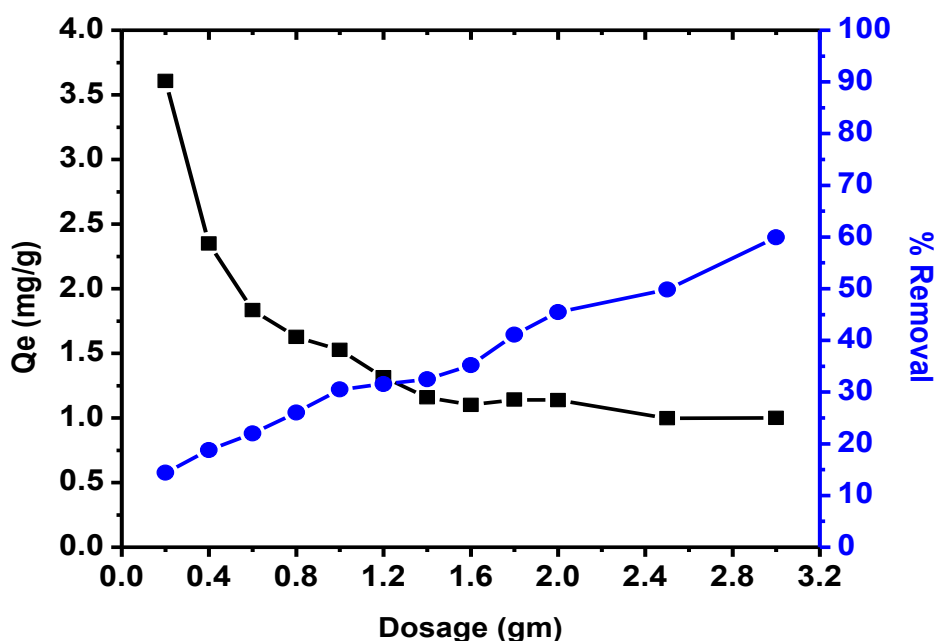


**Figure 4.15:** Graphical presentation of adsorbent dosage effect on adsorption process,  $V=50$  ml,  $C_0=100$  mg/g, adsorbent dose =0.2g to 3.0g, Stirring period =360 minutes, Natural pH,  $T = 25^\circ\text{C}$

It was found in the Fig.4.15 that with increase in ANC adsorbent dose the removal percentage increase but adsorption density decreases. The decrease in adsorption density can be attributed to the fact that some of the adsorption site remain unsaturated during the adsorption process, whereas the number of available adsorption site increases by an increase in adsorbent and this results in an increase in removal efficiency. Decrease of equilibrium concentration with the increasing of adsorbent doses for a given initial dye concentration, because for a fixed initial solute concentration, increasing the adsorbent doses provides a



greater surface area or adsorption site. The corresponding point on x-axis of the intersection point of these two curves give the optimal dose of adsorbent and here we found the optimal dose for AMC as 1.2g/ 50 ml (24 g/L) of RhB dye solution

#### 4.3.2 Effect of Contact time on RhB-ANC system

To investigate the effect of contact time was done based upon previously done technique. RhB dye ( $C_0=100$  mg/L), the batch experiments were carried out in a series of conical flasks with a constant ANC dose of 1.2 gm/50 ml in all the samples as optimal dose. These flasks were agitated in water bath shaker for 15, 30, 45, 60, 120,180,240,300 and 360 minutes at a constant 120 rpm at the natural pH and at 25<sup>0</sup>C in all the samples [29-33,37].

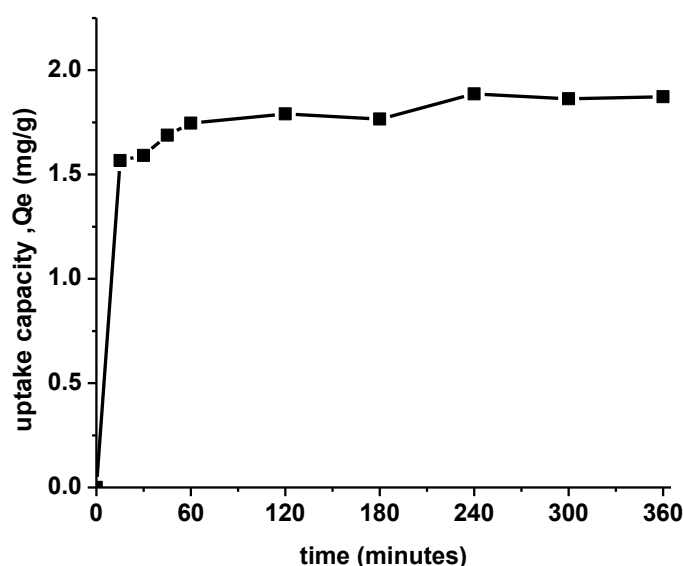


**Figure 4.16:** Time effect on adsorption process,  $V=50$  ml,  $C_0=100$  mg/g, Dose =1.2g/50 ml of dye solution, Stirring period =360 minutes, Natural pH,  $T = 25^{\circ}\text{C}$

In fig.4.16, it was shown that at 240 minutes the uptake capacity became constant, means it not changing with time, because it was the most sufficient time intimate interaction of sorbate-sorbent in RhB-ANC system. Therefore optimum time of adsorption for RhB-ANC system was found 240 minutes.

#### 4.3.3 Effect of pH on RhB-ANC system

As done previously in case of RhB-AMC case, same method was repeated. presence of several functional groups in the adsorbent decide the basic/acidic character to the adsorbent surface and causes the surface properties of ANC to depend on the pH of the aqueous solution.

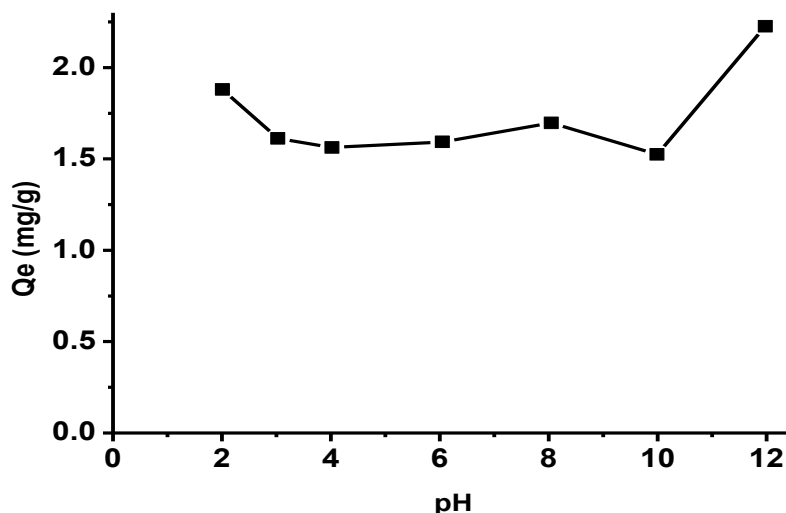


**Figure 4.17:** Graph of pH effect on adsorption process,  $V=50$  ml,  $C_0=100$  mg/g, Adsorbent dosage =  $1.2$  g/50 ml of dye solution, Stirring period = 240 minutes, pH = 2 to 12,  $T = 25^\circ\text{C}$

Here pH were set 2-12 with interval of 2 step, adsorbent dose was taken as  $1.2$  g in 50 ml of 100g/L concentration dye solution and whole experiment done at room temperature for 360 minutes with 120 rpm. Initially the uptake capacity was little high at pH 2 as shown in fig.4.17 then after the uptake capacity decreasing a little and remain retain constant uptake at range of pH 3~8. At pH 10 minimum uptakes was seen. Then after uptake capacity reached maximum at pH 12.

#### 4.3.4 Effect of point zero charge on RhB-ANC system

Point zero charge study was same as done previously in case of RhB-AMC system. Here in this case RhB-ANC system was taken. pH was set 2~12 with 1g of dose in 50 ml of 100mg/L concentration of dye solution. After pH were measures with pH meter after 24 hours of reaction of sorbate- sorbent.

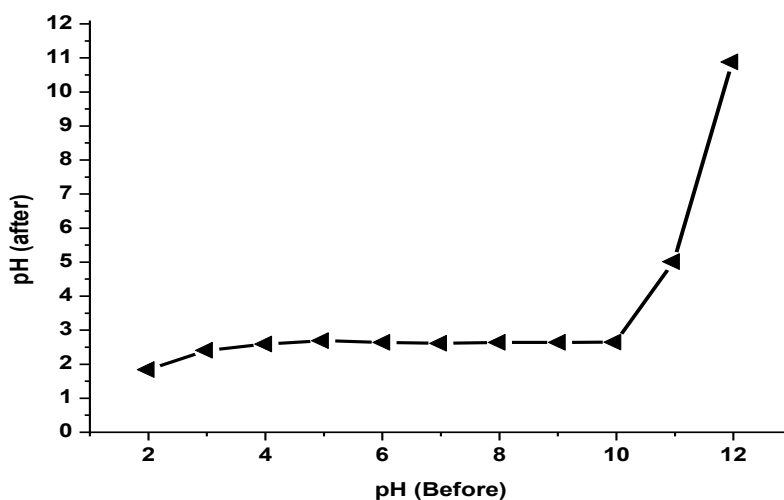


**Figure 4.18:** Graph of point zero charge,  $V=50$  ml,  $C_0=100$  mg/g, Dose =  $1$  g/50 ml of dye solution, Stirring time = 240 minutes, pH = 2 to 12 (maintained).  $T = 25^\circ\text{C}$

Final pH was measured and from fig.4.18  $pH_{zpc}$  of RhB dye-ANC system was found as 2.75. At  $pH < pH_{zpc}$ , the carbon surface has a net positive charge, while at  $pH > pH_{zpc}$  the surface has a net negative charge. The magnitude of surface charge of activated carbon decreases with increase in pH. Thus, electronegativity of activated increases with increase in pH. The lower removal of the positively charged dye at acidic pH range is probably due to the presence of excess  $H^+$  ions was competing with the dye molecule for the adsorption site. At alkaline pH, adsorbent surface gets net negative charge.

#### 4.3.5 Effect of initial concentration on RhB-ANC system

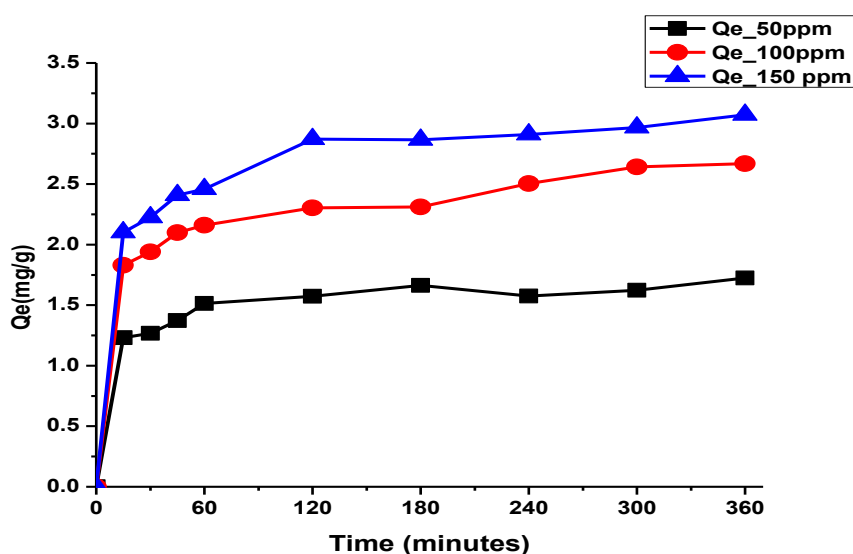


**Figure 4.19:** Graphical representation of initial concentration effect on adsorption process,  $V=50$  ml,  $C_0=100$  mg/g, Dosage = 1.2 g/50 ml of dye solution, Stirring time =240 minutes,  $pH = 12.0$  (maintained),  $T = 25^\circ C$

As done previously, three different concentrations as 50,100,150 mg/L of dye solution was taken for studies. Filtered supernatant was analyzed using spectrophotometer and a graph was plotted with  $Q_e$  versus time. The adsorption data for the uptake of phenol versus contact time at different initial concentrations is represented in Fig.4.18 below.

In Fig.4.19, showing that nearly 82% removal of dye with an initial concentration of 50 ppm and the equilibrium is reached 360 mins. However with initial concentration of 100 ppm about 64% removal is becoming possible and equilibrium was in the approaching state at the end of 360 mins and the results with the initial concentration of 150 ppm have shown 83% of dye removed and equilibrium achieved at 360 mins equilibrium. 50% of the total amount of dye uptake was found to occur in the first 45 minutes and the adsorption process was almost tending towards equilibrium at the end of 360 minutes. The higher sorption rate at initially may be due to an increased in concentration gradients between adsorbate in solution and adsorbate on adsorbent surface, as time precedes this concentration gradient is reduced due to

the accumulation of dye particles in the vacant sites leading to a decrease in the sorption rate at the larger stages from 45 to 360 minutes.

#### 4.3.6 Adsorption Kinetics

The different results were collected from these graphs. The contact time study can be used to determine the rate limiting step in the adsorption process with the help of a Weber –Morris plot. The possible rate limiting steps were mass transfer from the bulk liquid phase to the particle external surface, film diffusion and inter particle diffusion.

##### *Adsorption Kinetics for RhB- ANC System*

The time dependent batch adsorption data using fixed dose 1.2 gm with pH =12 maintained of adsorbent at 25 °C was used for kinetic modeling of the different dye system with an initial concentration of 1000 mgL<sup>-1</sup>

##### *4.3.6.1 Pseudo 1<sup>st</sup> order Kinetic model*

The linearized form of pseudo-first-order kinetics is given by equation (3.22) for RhB-ANC system and it is clear that, in figure 4.20 a plot of  $\ln(1-Ut)$  Vs. time should give a linear relationship with the slop  $K_1$  and intercept of  $\ln(q_e)$ .

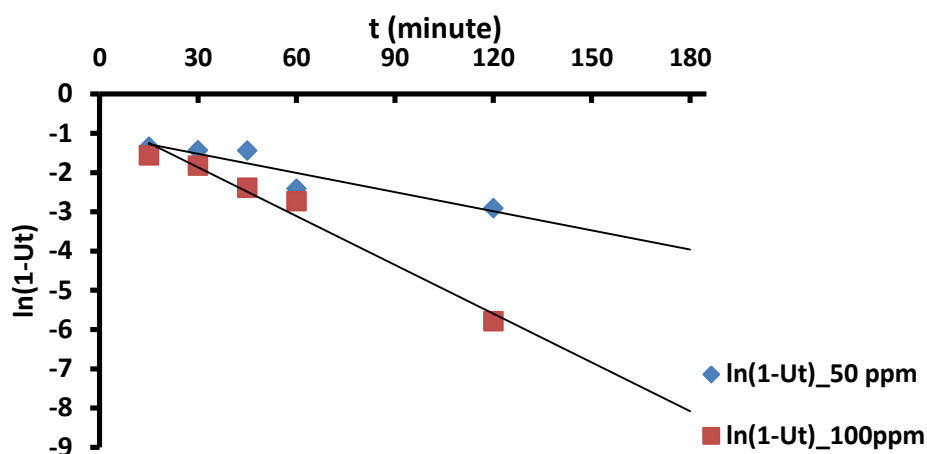


**Figure 4.20:** Pseudo first order kinetic model for RhB-ANC system; Dose = 1.2g/50 ml of dye solution,  $C_0$ = 50,100 and 150 mg/g, pH = 12

Table 4.7:Pseudo-first-order kinetic constants for RhB-ANC adsorption system					
$C_0$ (mg/L)	Kc	overall rate constant $K= K_1+ K_2$ (h <sup>-1</sup> )	Forward rate constant $K_1$ (h <sup>-1</sup> )	Backward rate constant $K_2$ (h <sup>-1</sup> )	R <sup>2</sup>
50	3.952	0.0163	0.0130	0.0033	0.8595
100	1.2457	0.0051	0.02297	-0.0179	0.6232

#### 4.3.6.2 Pseudo 2<sup>nd</sup> order Kinetic model

The linearized form of pseudo-second-order kinetics of RhB-ANC system is given by equation (3.24) in chapter 3. In figure 4.21 a plot of  $t(\text{time})$  Vs.  $t/Q_t$  should give a linear relationship with the slope  $1/q_t$  and with intercept of  $1/(K_2(q_t)^2)$

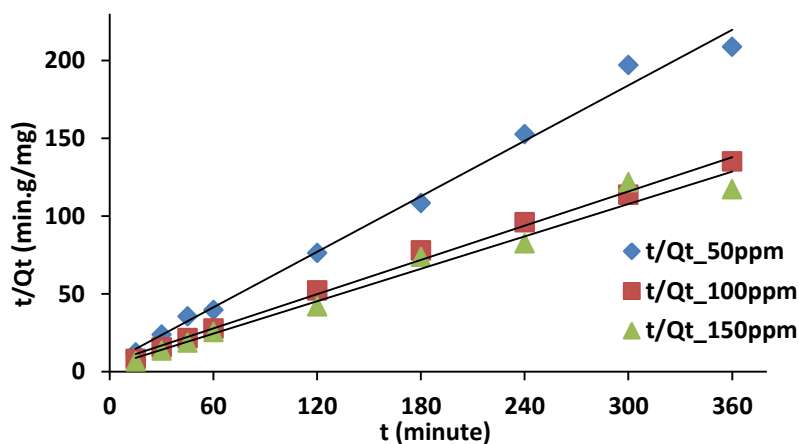


**Figure 4.21:** Pseudo second order kinetic model for RhB-ANC system

**Table 4.8:** Pseudo 2<sup>nd</sup> order kinetic model for RhB-ANC system

$C_0(\text{in ppm})$	$Q_e \text{ (mg/g)}$	$K_2$	$R^2$
50	1.68	0.063	0.992
100	2.726	0.023	0.996
150	2.883	0.033	0.974

#### 4.3.8 Effect of Temperature

In Endothermic process, adsorption capacity increases with temperature from fig.4.22, the adsorption capacity increases with temperature as  $35^\circ\text{C} < 45^\circ\text{C} < 55^\circ\text{C} < 65^\circ\text{C}$ .

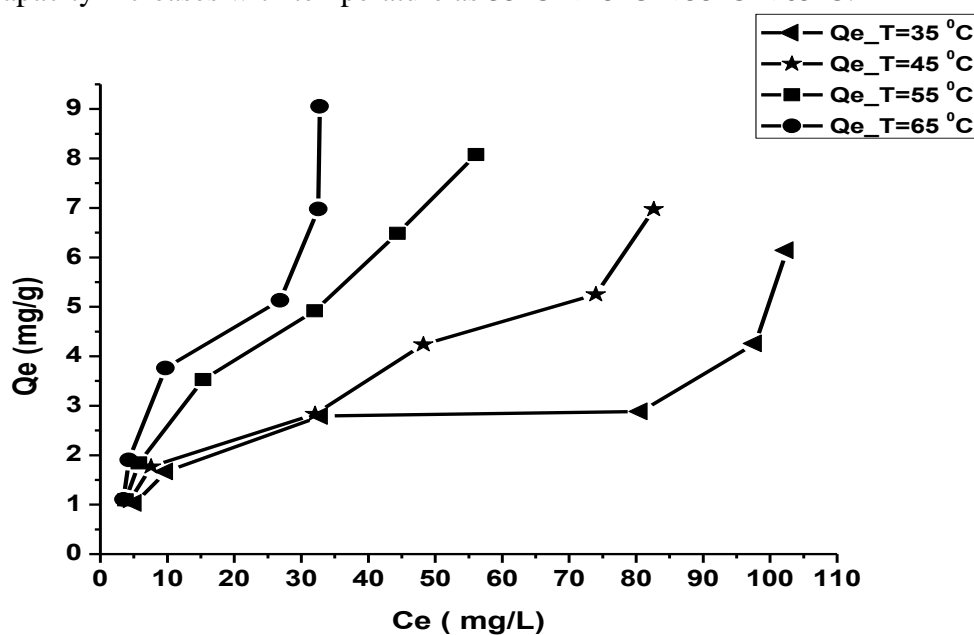


**Figure 4.22:** Adsorption equilibrium of different temperature for RhB –ANC system

#### 4.3.8 Adsorption equilibrium study for RhB - ANC system

For this equilibrium study, we have considered four basic isotherm models as same in previous system namely Langmuir, Freundlich, Temkin and D-R isotherm models.

##### i) Langmuir isotherm

The linearized form of Langmuir isotherm is given by equation 3.13 of chapter-3. The Langmuir Constant  $Q_0$ ,  $a_L$  and  $b_L$  can be calculated by plotting in the below figure 4.23 as  $C_t/Q_e$  vs.  $C_t$ .

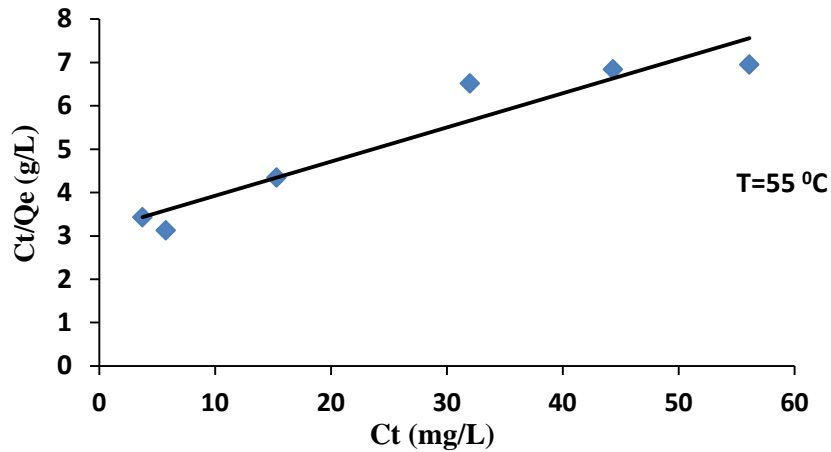


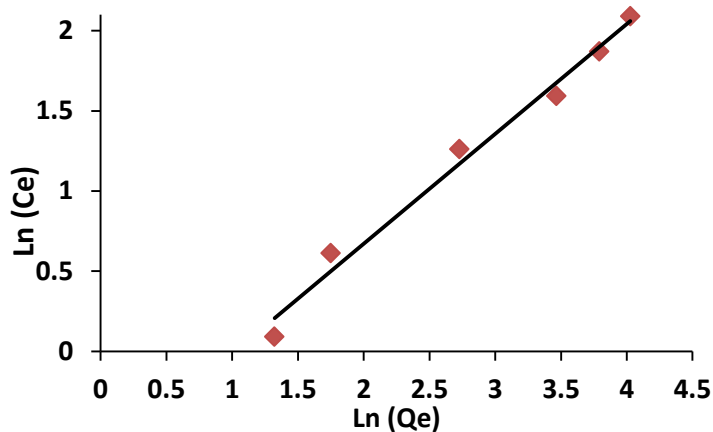
Figure 4.23: Langmuir isotherms for RhB-ANC system

Table 4.9: Langmuir isotherm parameters

Temp(°C)	$Q_{\max}$ (mg/g)	$b_L$ (mg/g)	$R^2$
35	5.674	0.0324	0.718
45	8.741	0.024	0.788
55	12.690	0.025	0.913
65	15.152	0.028	0.614

##### ii) Freundlich Isotherm

The linearized form of Freundlich isotherm for RhB-AMC system is given by equation 3.16 of chapter-3. The value of  $K_F$  and  $n$  can be calculated by plotting in figure figure 4.24 as  $\ln(Q_e)$  vs  $\ln(C_e)$ .



**Figure 4.24:** Freundlich isotherm for RhB-ANC system

**Table 4.10:** Freundlich isotherm parameters for RhB- ANC system

<i>Temp</i> (°C)	<i>n</i>	<i>K<sub>F</sub></i>	<i>R</i> <sup>2</sup>
35	2.087	0.495	0.887
45	1.776	0.489	0.962
55	1.459	0.497	0.986
65	1.332	0.551	0.932

### iii) Temkin Isotherm

The linearized form of Temkin isotherm is given by equation 3.18 of chapter-3. The value of  $K_T$  and  $B$  can be calculated by plotting in figure 4.25 as  $Q_e$  Vs.  $C_t$ .

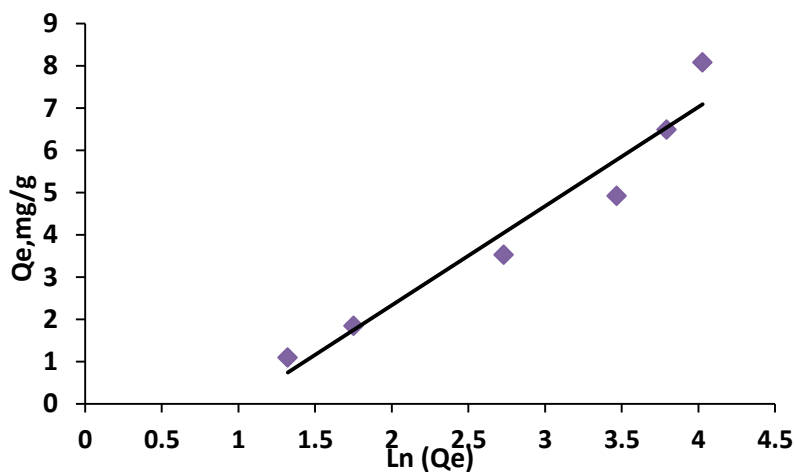


**Figure 4.25:** Temkin isotherm for RhB-ANC system

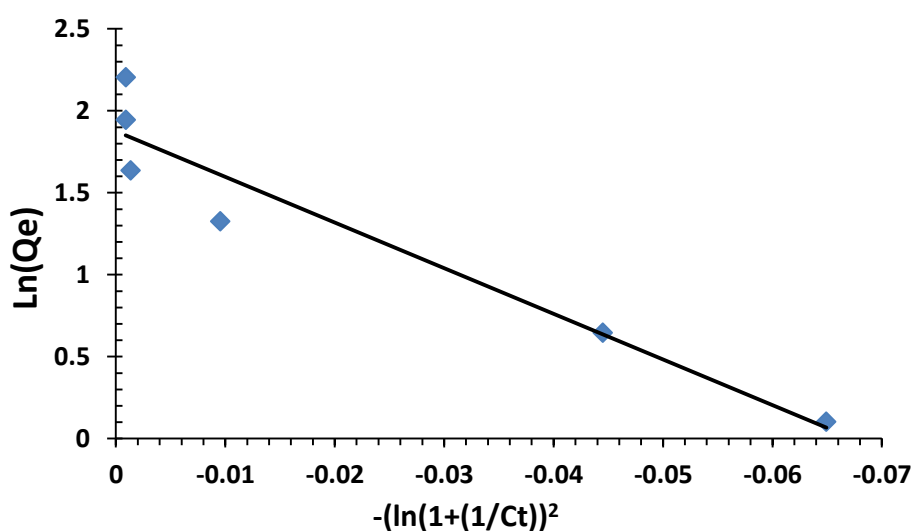
In the below table, Temkin isotherm parameters also calculated with different temperatures for RhB-ANC system

**Table 4.11:** Temkin isotherm parameters for RhB- ANC system

Temp(°C)	B	K <sub>T</sub>	R <sup>2</sup>
35	3.161	0.696	0.954
45	4.167	0.79	0.975
55	5.985	0.543	0.988
65	6.608	0.682	0.931

**iv) D-R Isotherm**

The linearized form of D-R isotherm is given by equation 3.19 of chapter-3. The value of  $\emptyset_D$  and  $\psi_D$  can be calculated by plotting in figure 4.26 as  $Q_e$  vs.  $C_t$ .

**Figure 4.26:** D-R isotherm studies for RhB- ANC system

In the similar way D-R isotherm plots for RhB-ANC adsorption systems at other temperatures were also made and the various parameters calculated from those plots were tabulated below.

**Table 4.12:** D-R isotherm parameter of RhB- ANC system

Temp(°C)	$\emptyset_D$	$\psi_D$	R <sup>2</sup>
35	3.668	49.109	0.747
45	4.399	36.378	0.775
55	5.558	31.843	0.865
65	6.526	27.856	0.920



## CHARACTERIZATION OF ADSORBENTS

---

### 5.1 THERMO GRAVITOMETRY ANALYSIS (TGA)

Thermo gravimetric Analysis (TGA) measures the amount and rate of change in the weight of a material as a function of temperature or time in a controlled atmosphere. Measurements are used primarily to determine the composition of materials and to predict their thermal stability at temperatures up to 1000°C. The technique can characterize materials that exhibit weight loss or gain due to decomposition, oxidation, or dehydration [43].

### 5.2 Fundamental of TGA

TGA study helps us in determining the range of pyrolysis temperature. A sharp bend in the curve shows the temperature at which the pyrolysis has to be started and the temperature at which the curve gets flat shows the end temperature of the pyrolysis. From figure 4, the range of pyrolysis was observed to be from 250 to 550 °C at 10°C/min and 250 to more than 600 °C at 20 °C/min. Initial stage, first stage decomposition represents the evaporation of moisture contents; Second decomposition indicates the formation of volatiles. During the Third stage, the pyrolysis residue slowly decomposed, with the weight loss velocity becoming smaller and the residue ratio tends to be constant at the end the decomposition of hydrocarbon. Due to high decomposition rate per unit time, the rapid decomposition zone or Second stage of decomposition is treated as active pyrolytic zone. During this stage, the intermolecular associations and weaker chemical bonds are destroyed. The side aliphatic chains may be broken and some small gaseous molecules are produced because of the higher temperature.

#### 5.2.1 TGA of Mahua seed

Here in case of raw Mahua seed, the material kept in temperature about 800 °C. With increases in temperature what is the effect of % mass is measured and calculated the best temperature for pyrolysis. In this graph, we can see that up to the 200 °C, the first stage of decomposition seen.

Again from temperature 200 °C to 400 °C, second stage of decomposition can be seen, which stage of volatile matter removed. Up to 650 °C the third stage of decomposition takes place. Temperature beyond 650 °C mass (%) being constant. Here we can choose the pyrolysis at temperature of 370 °C.

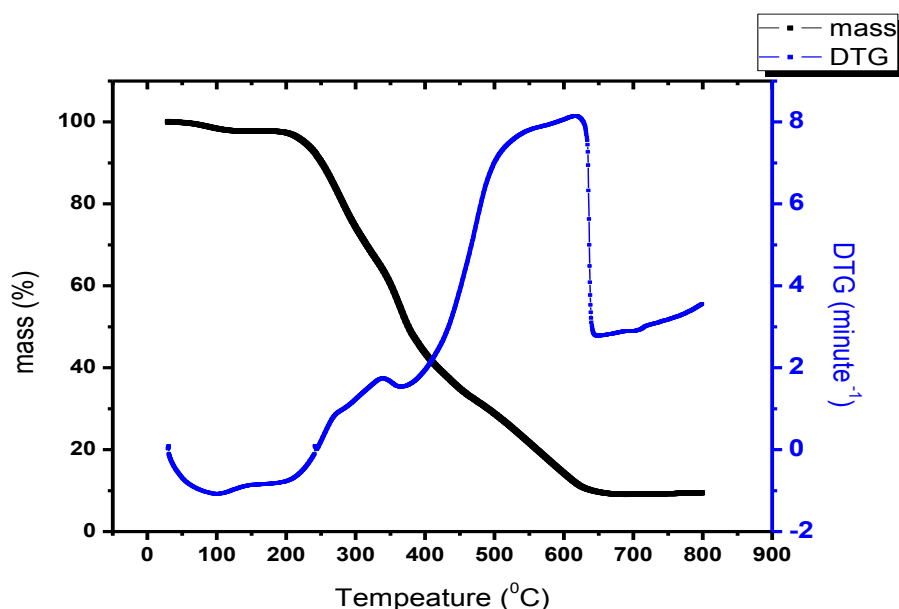


**Figure 5.1:** TGA of raw *Madhuca longfolia* (Mahua) seed

### 5.2.2 TGA of Aegle Marmelos (Bael )Shell

Here in case of raw aegle marmelos or bael shell, the material similarly kept up to 800 °C. With increases in temperature the % mass is changing. In this graph, we can see that up to the 250 °C, the first stage of decomposition seen. Again from temperature 250 °C to 350 °C, second stage of decomposition can be seen, in this stage of volatile matter removed. The third stage of decomposition can be seen at temperature range of 350 °C to 550 °C. Temperature beyond 550 °C shows constant mass (%) Here pyrolysis temperature for Bael shell is 390 °C.

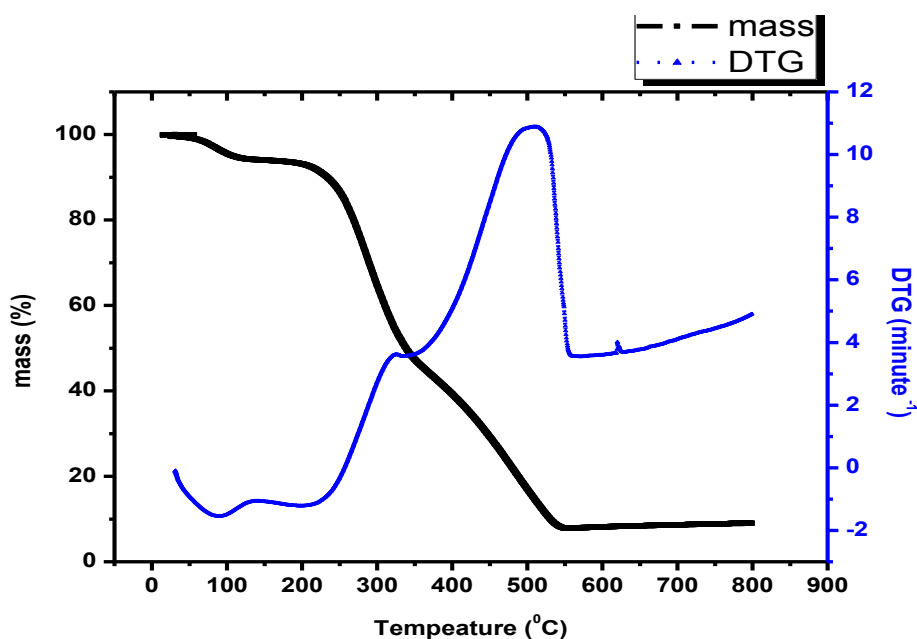


**Figure 5.2:** TGA of raw Aegle Marmelos (bael) shell

### 5.2.3 TGA of Neem Seed

Raw neem seed, the material for the preparation of adsorbent was kept for 800 °C. With increases in temperature the % mass was decreased. In this graph, we can see that up to the 250 °C, the first stage of decomposition seen. Again from temperature 250 °C to 330 °C, second stage of decomposition can be seen, in this stage of volatile matter removed. The third stage of decomposition can be seen at temperature range of 330 °C to 630 °C. Temperature beyond 630 °C shows constant mass (%) Here pyrolysis temperature for Neem seed is 400 °C.

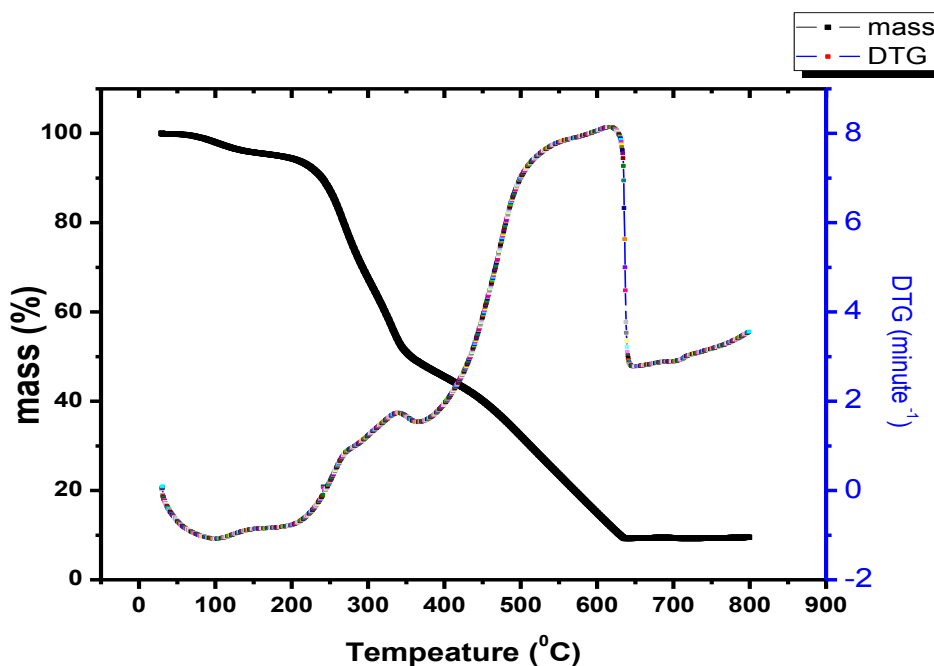


**Figure 5.3:** TGA of raw *Azadirachta indica* (Neem) Seed

### 5.2.4 TGA of Abrus Precatorius Seed

*Abrus precatorius* seed taken for TGA. With increases in temperature the mass % was decreased (started from 100 %). Hemicellulose will decompose at temperature 200- 250 °C, cellulose in 250-350 °C, and lignin between temperature 300 and 500 °C [43]. The DSC curve shows the parts with endothermic and exothermic reactions. Near 100 °C, endothermic reaction is observed because heat is supplied for the removal of moisture. Pyrolysis range was observed to be from 250 to 600 °C at 10°C/min and 250 to more than 800 °C at 20 °C/min. In this case the first stage decomposition represents the evaporation of moisture contents; Second decomposition indicates the formation of volatiles. During the Third stage, the pyrolysis residue slowly decomposed, with the weight loss velocity becoming smaller and smaller and the residue ratio tends to be constant at the end the decomposition of

hydrocarbon. Due to high decomposition rate per unit time, the rapid decomposition zone or Second stage of decomposition is treated as active pyrolytic zone.

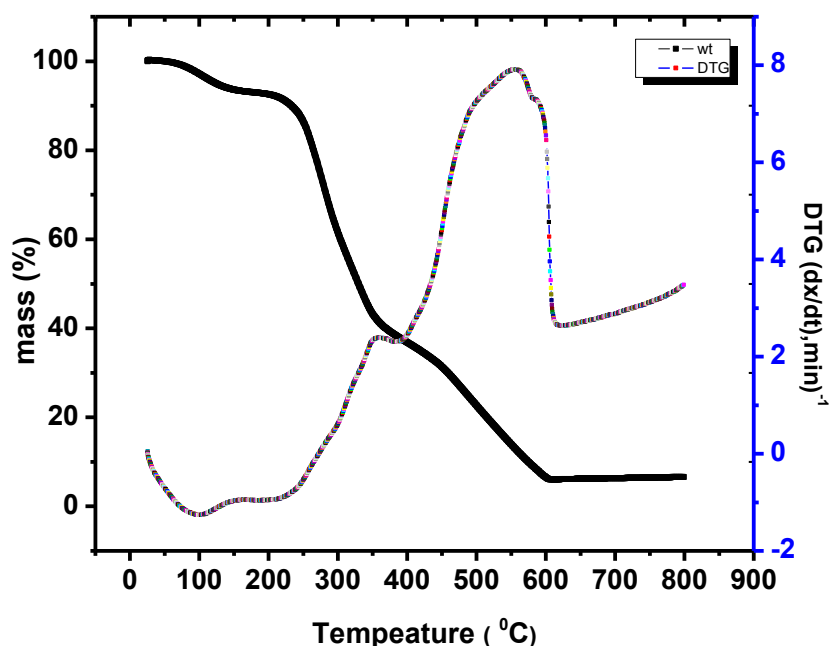


**Figure 5.4:** TGA of raw *Abrus Precatorius* (Crab's eye) seed

### 5.3 PROXIMATE ANALYSIS

Proximate analysis is one the standard method of physicochemical characterization of the adsorbents. It was developed as a simple means of determining the distribution of products obtained when the coal sample is heated under specific condition. These conditions are strictly according to the ASTM standard of coal heating. As per the definition by ASTM D-3172 Proximate analysis of coal separates the product into four groups :(i)Moisture, (ii) Volatile matter, consisting of gases and vapour driven off during pyrolysis (iii) Fixed carbon, the non-volatile fraction of coal :and (iv)Ash, the inorganic residue remaining after combustion.

The standard test method for proximate analysis covers the methods of analysis associated with the proximate analysis of the coal and coke and is, in fact, a combination of determination of each of the three of the properties and calculation of the fourth. Moisture, Volatile Matter and ash content are all determined by subjecting the coal to prescribe temperature levels for prescribe time intervals. The losses of weight are, due to loss of moisture and, at the higher temperature, loss of volatile matter. The residue remaining after ignition at the final temperature is called ash. Fixed carbon is the difference of these three values summed and subtracted from 100. In low volatile materials such as coke, the fixed

carbon value equates approximate to the elemental carbon content of the sample. Proximate analysis gives quick and valuable information regarding commercial classification and determination of suitability for particular industrial use.

**(i) Moisture Content**

Moisture Content generally increases the transportation load and cost and the calorific value reduces. 10 grams of char sample taken in a Petridis and kept it in oven at 105-110 °C for 1.5 hours. Then after the sample taken out and put in the desiccator. After certain time the dried sample weighted and percentage of moisture content was calculated.

**(ii) Volatile Matter**

A known amount of sample was put in a crucible. The crucible was placed in a muffle furnace at 900 °C + 10 °C, covered with lid, and placed for exactly 7 minutes. The crucible was taken out, allowed to cool and weighed.

**(iii) Ash**

The crucible was ignited in the muffle furnace at 650 + 25 °C for 1 hour. The crucible was placed in the desiccator, cooled to room temperature and weighed. A known amount of the sample which was dried in the hot air oven at 150 °C for 3 hours was put in the crucible and the crucible was placed back in the muffle furnace at 650 + 25 °C for 3 hours. The crucible was taken out of the furnace, placed in the desiccator, cooled to room temperature and weighed.

**(iv) Fixed Carbon**

Fixed carbon ( FC) =100-(volatile matter + ash content+ moisture content)

**Table 5.1 Proximate Analysis data (%) (Dry basis)**

<i>% of Compound</i>	<i>Moisture</i>	<i>Ash</i>	<i>Volatile Matter</i>	<i>Fixed carbon</i>
Activated Abrus Precatorius	11.91	1.73	28.09	58.27
Activated Neem Carbon	3.59	5.00	32.14	59.27
Activated Aegle Marmelos Carbon	2.33	7.13	32.54	58.00
Activated Mahua Carbon	3.50	5.90	28.77	56.83

### Ultimate Analysis (Dry basis)

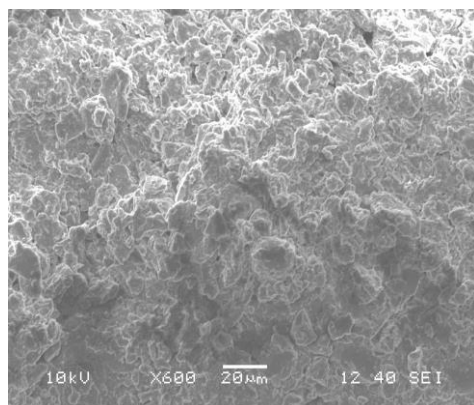
**Table 5.2** Ultimate Analysis data (%) (Dry basis)

<i>Adsorbent Name</i>	<i>% Composition of Elements</i>					
	<i>C</i>	<i>H</i>	<i>N</i>	<i>S</i>	<i>O</i>	<i>Ash</i>
Activated Abrus Precatorius Carbon	60.77	3.53	4.02	1.20	28.75	1.73
Activated Neem Carbon	63.21	4.87	4.55	0.81	21.57	5.00
Activated Aegle Marmelos Carbon	61.35	4.84	3.77	1.54	21.37	7.13
Activated Mahua Carbon	58.98	6.42	4.01	1.15	23.54	5.90

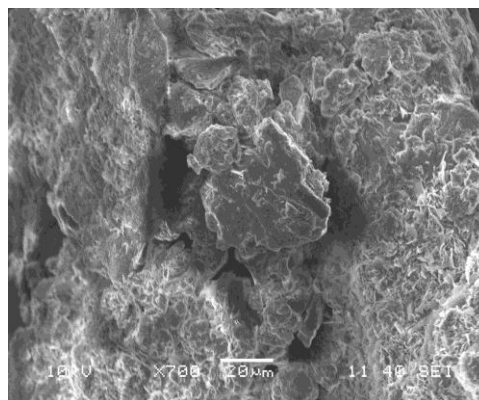
## 5.4 SEM (Scanning Electron Microscope)

SEM studies stands for scanning electron microscopy, which is used for studying the surface morphology of substances due to its high magnification imaging capability. Scanning electron microscopy images were taken by using JEOL (JSM-6480LV) microscope having an acceleration voltage of 15 kV.

### 5.4.1 SEM of Activated Mahua Carbon (AMC)



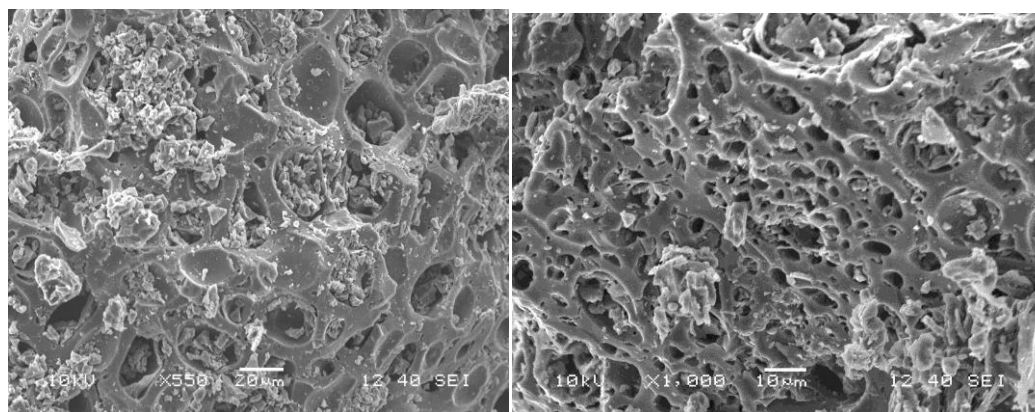
**SEM of AMC a) 600X**



**b) 700X**

Investigating SEM, surface morphology, it can be clearly seen that in case of 600X and 700 X magnifications that the surface pores are uniformly distributed. The distribution of pores in activated carbons can vary significant depending upon the raw material. The different shape of pore with different of raw material. The pore size distribution also affects the efficiency and selectivity of adsorption. A consideration of the dimensions of some pollutants shows that activated carbon can feasibly be used to remove many of the impurities occurring in water.

#### 5.4.2 SEM of Activated Aegle Marmelos Carbon (AAM)

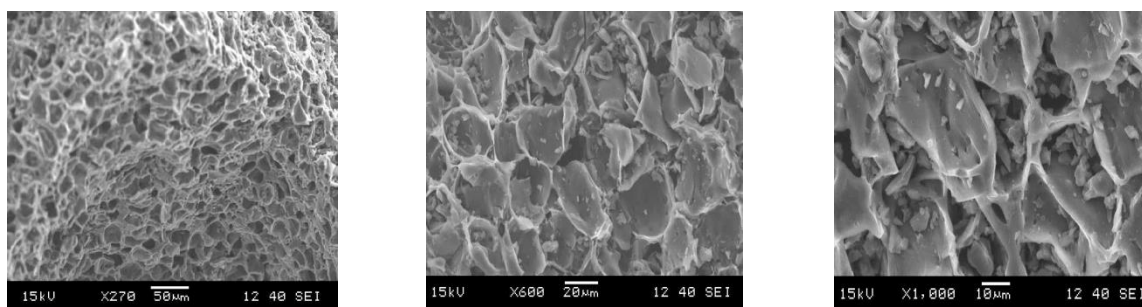


SEM of ABC a) 600X

b) 1000X

By investigating the surface morphology of activated mahua carbon by SEM, the analysis was done at two different magnification namely 600X and 1000X respectively. Here we can clearly visualize the pore size uniformity of adsorbent. The pore openings at 600X magnification shows that pore of the surface bubbled out, describing a sudden burst due to rapid thermal expansion. Further at higher magnification. At a higher magnification i.e. 1000X it was seen that the pores build-up was found to be very clear opening that provide accessibility into internal pores and high surface area essential for the adsorption purposes.

#### 5.4.3 SEM figure of Activated Abrus precatorius (AAP)



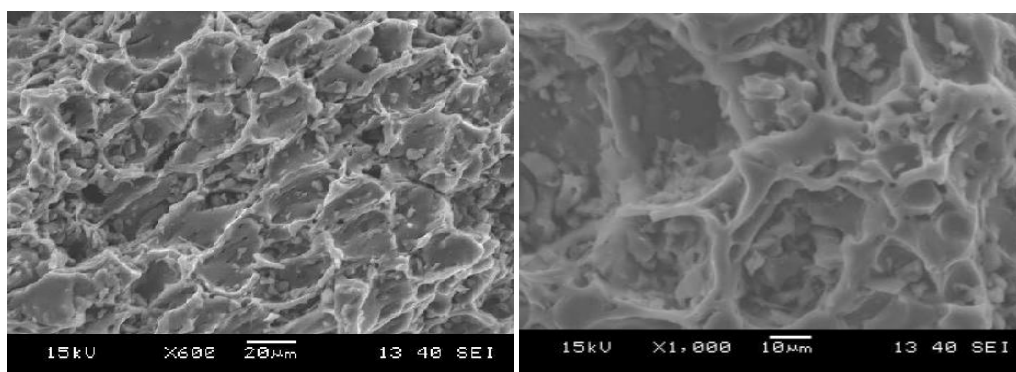
SEM of GAC , (a) 270X

(b) 600 X

(c) 1000X

For studying the surface morphology of AAP, analysis was done at three different magnifications namely 270, 600 and 1000X respectively. In all figure, it can be notice that the pore size distribution is uniform which a prime goal of a good adsorbent. The image shows heterogeneous distribution of pores and rough texture on the surface of AAP. The pore openings at 600X magnification shows that pore of the surface bubbled out, describing a sudden burst due to rapid thermal expansion. Further at higher magnification. At a higher magnification i.e. 1000X it was seen that the pores build-up was found to be very clear opening that provide accessibility into internal pores and high surface area essential for the adsorption purposes.

#### 5.4.4 SEM of Activated carbon Neem seeds(ANC)



SEM of ANC (a) 600 X

(b) 1000X

Similarly SEM analysis was done for ANC at different magnifications namely 600X and 1000X respectively. At lower magnification the image showed detailed external morphology with macropores on their surfaces, and it is also revealed from the figure that uniformity of pore is there. At a two times higher magnification i.e. at 1000X, one can easily visualize the fibrillar arrangement of ANC which were of course producing better adsorption possibility.

#### 5.5 BET ANALYSIS

In case of gas adsorption, both the Adsorption and desorption at any clean surface of dry solid powder as well as the pore size distribution of porous materials. In an experiment of gas sorption, the material is being heated and degassed by vacuum force or inert gas, such as N<sub>2</sub>, krypton or alternatively withdrawn and desorbed. The sample material is placed in a vacuum chamber at a very low constant temperature, generally at the temperature of liquid nitrogen (77.4 K) and it operated at a wide range of pressure for generating adsorption and desorption isotherms. The amounts of gas molecules adsorbed or desorbed are determined by the pressure variations due to adsorption and desorption of the gas molecules by adsorbent.

**Table 5.3 : BET analysis data of four different materials**

Name of Material / adsorbent	Adsorbent External surface area, m <sup>2</sup> /g
Activated Mahua Carbon (AMC)	137
Activated Neem Carbon (ANC)	234.6
Activated Aegle Marmelos Carbon (AMC)	169.2
Activated Abrus Precatorius Carbon (APC)	228.6

Various amount of gas molecules will be adsorbed or desorbed at different doses of the gas (the adsorbate). Total surface area of the material can be determined by knowing the area occupancy of a single adsorbate. Both single point and double point method is used to find



the surface area. Most widely used method of determining the surface area is BET nitrogen adsorption method. The multipoint as 5 points, 10 points, 20 points and etc. can be calculated. BET method is used to measure total surface area.

## **5.6 Fourier Transform Infra-Red spectroscopy (FTIR)**

Fourier Transform Infrared spectroscopy (FTIR) is an important analysis technique that detects various characteristic functional groups available in any solid or liquid sample. Basically it is a spectroscopic analysis technique which is used for identification of chemical bonds in a molecule by producing an infrared absorption spectrum and from there of the functional groups present on the surface of sample. Interaction of an infrared light with Activated carbon the chemical bond will stretch, contract, and absorb infrared radiation in a specific wave length range in the presence of the rest of molecules. Based on this, the principle functional groups present in the activated biomass carbon were identified. During analysis the sample is irradiated by infrared radiations, some of the infrared radiations are absorbed by the sample and rest are passed (transmitted) through. The FTIR spectra were collected generally in the range of  $400\text{--}4000\text{ cm}^{-1}$  region with  $8\text{ cm}^{-1}$  resolution. Absorption in the infrared region makes changes in vibrational and rotational status of the molecules. The absorption frequency depends greatly on the vibrational frequency of the molecules. The absorption intensity depends on how the infrared photon energy can be transferred to the molecule. This depends on the change in the dipole moment that occurs as a result of molecular vibration. A molecule will absorb infrared light only if the absorption causes a change in the dipole moment.

All compounds except for elemental diatomic gases such as  $\text{N}_2$ ,  $\text{H}_2$  and  $\text{O}_2$ , have infrared spectra and most components present in a flue gas is also analysed by their characteristic infrared absorption. If only one species is analysed, a species-specific instrument can also be used. Analysis is carried out in a narrow wavelength interval, where the species of interest has a characteristic absorption. Other components present in the sample also absorb at the analytical wavelength, so the spectrometer should be calibrated for cross sensitivities. Quantification of several components absorbing in the mid infrared region ( $400\text{--}5000\text{ cm}^{-1}$ ), either conventional dispersive infrared analysis or Fourier Transform Infrared (FTIR) spectroscopy can also be used. Compared to dispersive IR analysis, FTIR analysis is faster and has a better signal to noise ratio.

This spectrum represents a fingerprint of the sample with absorption peaks corresponding to the frequencies of vibrations between the bonds of the atoms which make up the material. Thus, it gives an idea about the organic functional groups present in the sample. The samples

were usually prepared with KBr, in the form of pellets. FTIR analysis is done using the instrument FTIR analyzer by Shimadzu IR Prestige-21, Manufacture in Japan.

#### (i) FTIR analysis of Virgin AMC and dye loaded AMC

The IR spectra of the treated virgin activated mahua carbon seed and dye loaded carbon were presented in fig.5.5.

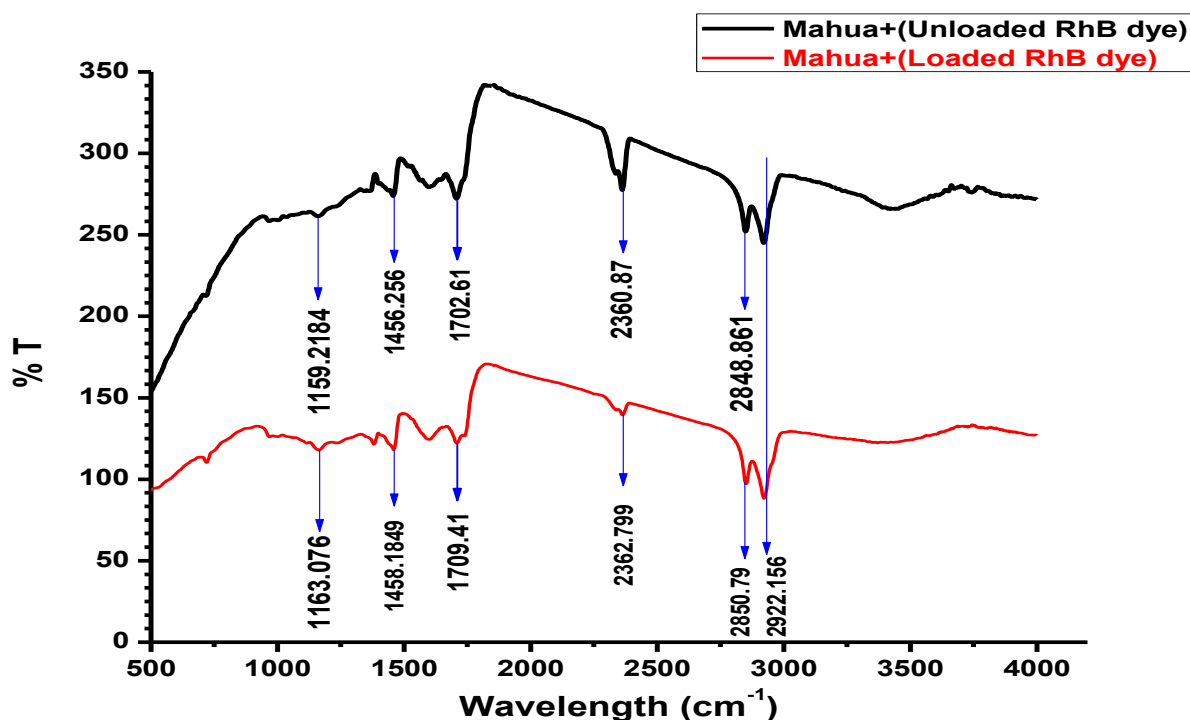


**Figure 5.5:** FTIR analysis of virgin AMC and RhB dye loaded AMC

Region between 3200-2700  $\text{cm}^{-1}$  indicates for organics and hydrocarbon, in this region are normally characteristics of carbon and hydrogen containing species which are assigned to various forms of C-H stretching. Peak no.2922.156  $\text{cm}^{-1}$  Characteristic of carbon-and hydrogen containing species, with single bond and are assigned to various forms of C-H stretching,  $\text{CH}_3$ , Alkane. It can be inferred that the alkane group do not play any significant role in adsorption, means peak remain unchanged. Peak 2848.861  $\text{cm}^{-1}$  characteristic of carbon-and hydrogen containing species, with double bond and are assigned to various forms of C-H stretching,  $\text{CH}_2$ , Alkene. After RhB dye adsorption peak shifted to 2850.79 $\text{cm}^{-1}$ . Peak 2360.87 $\text{cm}^{-1}$ , characteristic of carbon-and hydrogen containing species, with single bond and are assigned to various forms of C-H stretching, dye loaded AMC shifted to 2362.87. Peak no.-1702.61 $\text{cm}^{-1}$  characteristic of carbon and oxygen containing species and are assigned to various forms of C double bond with oxygen stretching,  $=\text{C}=\text{O}$  group(carboxylic group) and after loading of dye it shifted to 1709.41 $\text{cm}^{-1}$ . Peak no.-1456.25  $\text{cm}^{-1}$ , characteristics of

methane bending and are assigned to form of C-H bending, CH<sub>2</sub> group, after dye loading shifted to 1458.18 cm<sup>-1</sup>.

The presences of these groups are responsible for adsorption of RhB dye on to the Activated Mahua seed carbon ,AMC (adsorbent) surface.

## (ii) FTIR analysis of Virgin ANC and dye loaded ANC

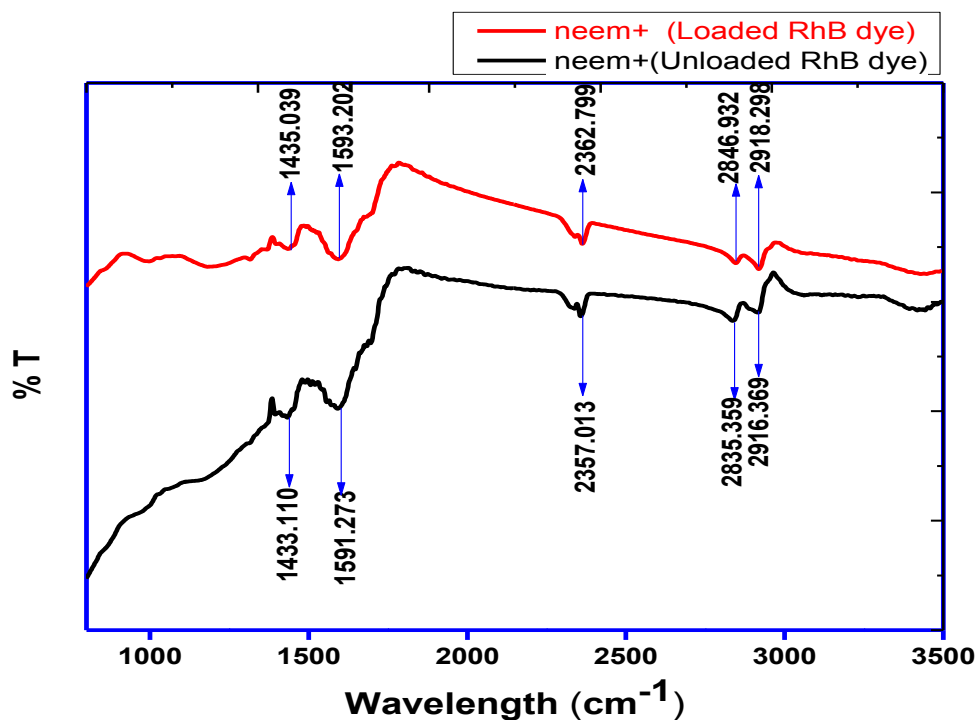


**Figure 5.5:** FTIR analysis of virgin ANC and RhB dye loaded ANC

It can be inferred that the alkane groups do play a significant role in adsorption as their adsorption peak 2916.3 cm<sup>-1</sup> shifted to 2918.3 cm<sup>-1</sup> by dye adsorption. Peak 2835.3 cm<sup>-1</sup> adsorption peak shifted to 2846.9 cm<sup>-1</sup>. Due to the presence of double bond and are assigned to various forms of C-H stretching, CH<sub>2</sub>, alkene. Peak 2357.01 cm<sup>-1</sup>, characteristic of carbon- and hydrogen containing species, with single bond and are assigned to various forms of C-H stretching, dye loaded AMC shifted to 2362.79 cm<sup>-1</sup>.

The peak 1591.27 cm<sup>-1</sup> is attributed to NH<sub>2</sub> scissoring vibration, which after adsorption with RhB dyes as a single sharp peak at 1593.20 cm<sup>-1</sup>. There by proving that the NH<sub>2</sub> group are also responsible for the adsorption of dye Change also appear in the carboxylic band which now appears at 1593.2 cm<sup>-1</sup> ,before adsorption it was 1591.2 cm<sup>-1</sup>.Peak no.-1433.1cm<sup>-1</sup>, characteristics of methane bending and are assigned to form of C-H bending, after dye loading shifted to 1435.03 cm<sup>-1</sup>.

Presence of all these groups are intensely responsible for adsorption of RhB dye on to activated neem seed carbon, ANC,(adsorbent).

## CONCLUSION

Removal of Rhodamine B (RhB) dye from aqueous solutions by adsorption using activated carbon prepared from *Madhuca longfolia* (activated mahua seed carbon) and *Azadirachta indica* (activated neem seed carbon) seed has experimentally determined. The prepared different four activated carbons were characterized by different analysis and test.

For this whole project work, activated mahua seed carbon (AMC) and activated neem seed carbon (ANC) were chosen among four self-prepared adsorbents and adsorption studies were done, because of these two materials having low and high BET surface area respectively along with other characterization analysis. It was also found that, AMC and ANC were most suitable for better adsorption with minimal cost with adverse effect.

The following conclusions are derived from the experimental investigation

- Among four self-prepared adsorbents in the laboratory, higher percentage (%) of carbon content were found as followed,  $ANC > AAM > AAP > AMC$ .
- Chemical activation of precursor by ortho-phosphoric acid with 40% impregnation gave better adsorbent surface morphology nature
- BET Surface area as a characterization parameter of AMC and ANC was confirmed the mesoporous texture, highly carbonaceous nature and a higher effective multi-layer adsorption using  $N_2$  as surface area of  $137\text{ m}^2/\text{g}$  and  $234.6\text{ m}^2/\text{g}$  respectively.
- Point Zero charge ( $pH_{pzc}$ ), of AMC and ANC were determined as 6.0 and 2.75 respectively. At this pH the adsorbent surface's net charge become zero.

### For RhB-AMC system

- The maximum adsorption capacity of dye was found to  $39.683\text{ mg/g}$
- $M = 10\text{ g/L}$  as optimum adsorbent dose,  $t = 3$  hours as optimum contact time up to the getting of constant adsorption.
- Uptake capacity increases with increase in dye concentration with the increase of time interval in initial concentration effect
- $H^+$  concentration for this system set as pH 4, means that experiments did in acidic medium.
- At Temperature  $65^\circ\text{C}$  maximum adsorption or removal took place in endothermic condition In case of RhB- AMC, maximum removal 94.67 % achieved with having operation variable as followed,  $pH = 4$ , adsorbent dose  $10\text{ g/L}$ ,  $C_0 = 30\text{ mg/L}$ ,  $V = 50\text{ ml}$ , optimum contact time was 180 minutes with 120rpm of shaker and temperature at  $65^\circ\text{C}$

- The kinetics studies confirmed that RhB -AMC adsorption system can be described by Pseudo-second-order kinetic model
- For best fitting to adsorption isotherms, the values of it compared with linearity by  $R^2$  value, which showed as, freundlich > Temkin > Langmuir > D-R isotherm

### **For RhB-ANC system**

- The maximum adsorption capacity of dye was found to 15.152 mg/g.
- For RhB-ANC system optimum adsorbent dose,  $M = 24$  g/L,  $t = 4$  hours as sufficient time for maximum removal and mixing of dispersed solution
- As pH is a most influencing parameter and  $pH = 12$  set as optimum value, adsorption for this system took place in basic environment
- Increasing of time give a consecutive higher value uptake capacity up to a certain period and then became constant. Uptake capacity increase with increase of initial dye concentration
- At Temperature  $65^\circ\text{C}$  maximum dye removal took place in endothermic condition
- In case of RhB- ANC, maximum removal 91.5 % achieved with having operation variable as followed,  $pH = 12$ , adsorbent dose 24 g/L,  $C_0 = 50$  mg/L,  $V = 50$  ml, optimum contact time was 240 minutes with 120 rpm of shaker and temperature at  $65^\circ\text{C}$
- The kinetic of adsorption followed the pseudo second order kinetic model.
- For best fitting to adsorption isotherms, the values of it compared with linearity by  $R^2$  value, which showed as, freundlich > Temkin > D-R isotherm > Langmuir isotherm

## **FUTURE WORK**

The following recommendation to be done for further studies

- Adsorption studies of RhB( basic dye) using other self-prepared or commercial adsorbents
- More detail characterization of self-prepared adsorbents must be perform
- Optimization of process/operation variables using statistical method
- Adsorption studies will investigate through the *continuous flow system* method and fluidized bed system also be performed for best utilization of this adsorption process
- RhB dye desorption studies will also be perform.

## REFERENCE

1. Selvam P.P., Preethi S., Basakara lingam P., Thinakaran N., Sivasamy A., Sivanesan S., (2008), “Removal of Rhodamine B from aqueous solution by adsorption onto sodium montmorillonite”, *Journal of Hazardous Materials* 155 (2008) 39–44
2. Haddad M.E., Mamouni R., Saffaj N., Lazar S., (2012), “Adsorptive Removal of Basic Dye Rhodamine B from Aqueous Media onto Animal Bone Meal as New Low Cost Adsorbent”, *Global Journal of Human Social Science, Geography & Environmental Geo Sciences*, Volume 12 Issue 10 Version 1.0 Year 2012
3. Vijayakumar G., Tamilarasan R., Dharmendra kumar M., (2012), “Adsorption, Kinetic, Equilibrium and Thermodynamic studies on the removal of basic dye Rhodamine-B from aqueous solution by the use of natural adsorbent perlite”, *J. Mater. Environ. Sci.* 3 (1) (2012) 157-170
4. Yan X.H. and Prasad M., (2009), “Discoloration of Rhodamine B dyeing wastewater by schorl-catalyzed Fenton-like reaction”, *Sci China Ser E-Tech Sci*, Oct. 2009, vol. 52, Number. 10, 3054-3060
5. Maurya N.S., Mittal A.K., and Cornel P., (2008), “Evaluation of adsorption potential of adsorbents: A case of uptake of cationic dyes”, *Journal of Environmental Biology* January 2008, 29(1) 31-36 (2008)
6. Namasivayam C. and Yamuna R.T., (1991), “Removal Of Rhodamine-B By Biogas Waste Slurry From Aqueous Solution”, Received July 27, 1991; revised November 8, 1991
7. Gupta V. K., Suhas, Ali Imran and Saini V. K., (2004) “Removal of Rhodamine B, Fast Green, and Methylene Blue from Wastewater Using Red Mud, an Aluminum Industry Waste”, *Ind. Eng. Chem. Res.* 2004, 43, 1740-1747
8. Auta M., (2012), “Fixed Bed Adsorption Studies Of Rhodamine B Dye Using Oil Palm Empty Fruits Bunch Activated Carbon”, *Journal of Engineering Research and Studies (JERS)*, Vol. III, Issue III, July-Sept, 2012/03-06
9. Li L., Liu S., Zhu T., (2010), “Application of activated carbon derived from scrap tires for adsorption of Rhodamine B ”, *Journal of Environmental Sciences* 2010, 22(8) 1273–1280
10. Parimaladevi P. and Venkateswaran V., (2011), “Adsorption Of Cationic Dyes (Rhodamine B And Methylene Blue) From Aqueous Solution Using Treated Fruit Waste”, *Journal of applied technology in Environmental Sanitation*, Volume 1 , Number 3 : 285 -293 , October , 2011

11. Inbaraj B.S., Sulochana N., (2006), "Use of jackfruit peel carbon for adsorption of rhodamine B, a basic dye from aqueous solution", Indian Journal of Chemical Technology, Volume 13, January 2006, pp. 17-23
12. Annadurai G, Juang R.S., Lee D.J., "Use of cellulose-based wastes for adsorption of dyes from aqueous solutions", Journal of Hazardous Materials B92 (2002) 263–274
13. Gupta V.K., Jain R., Siddiqui N., Saleh T.A, Agarwal S., Malati S. and Pathak D., (2010), "Equilibrium and Thermodynamic Studies on the Adsorption of the Dye Rhodamine-B onto Mustard Cake and Activated Carbon", J. Chem. Eng. Data 2010, 55, 5225–5229
14. Hema M., Arivoli S., "Rhodamine B adsorption by activated carbon: kinetic and equilibrium studies", Indian Journal of Chemical Technology, Volume 16, January 2009, pp. 38-45
15. Sivaraj R., Venckatesh R., Gowri, Sangeetha G., (2010), "Activated carbon prepared from *eichornia crassipes* as an adsorbent for the removal of dyes from aqueous solution", International Journal of Engineering Science and Technology, Vol. 2(6), 2010, 2418-2427
16. Aliabadi M., Khazaei I., Hajiabadi M, Fazel S., (2012), "Removal of rhodamine B from the aqueous solution by almond shell biosorbent", J. Bio. & Env. Sci. , Vol. 2, Number- 9, pp. 39-44, 2012
17. Mohammadi M., Hassani A.J., Mohamed A.R., and Najafpour G.D., (2010), "Removal of rhodamine b from aqueous solution using palm shell-based activated carbon: adsorption and kinetic studies" J. Chem. Eng. Data 2010, 55, 5777–5785
18. Khan T.A., Sharma S. and Ali I., (2011) "Adsorption of Rhodamine B dye from aqueous solution onto acid activated mango (*Mangifera indica*) leaf powder: Equilibrium, kinetic and thermodynamic studies", Journal of Toxicology and Environmental Health Sciences Vol. 3(10), pp. 286-297, 14 September, 2011
19. Das S.K., Bhowal J., Das A.R., and Guha A.K., (2006), "Adsorption Behavior of Rhodamine B on *Rhizo pusoryzae* Biomass", Langmuir 2006, 22, 7265-7272
20. Jaina R., Mathura M., Sikarwara S., Mittal A., (2007), "Removal of the hazardous rhodamine B dye through photo catalytic and adsorption treatments", Journal of Environmental Management, 85 (2007) 956–964
21. Theivarasu C., Mysamy S., (2010), "Equilibrium and Kinetic adsorption studies of Rhodamine B from aqueous solutions using cocoa shell as a new adsorbent", International Journal of Engineering Science and Technology, Vol. 2(11), 2010, 6284-6292

22. Venkatraman B.R., Gayathri U., Elavarasi S., and Arivoli S., (2012), "Removal of Rhodamine B dye from aqueous solution using the acid activated *Cynodon dactylon* carbon", *Der Chemica Sinica*, 2012, 3(1):99-113
23. Ahamed A.J., Balakrishnan V. and Arivoli S., (2011), "Kinetic and equilibrium studies of the Rhodamine B adsorption by low cost activated carbon", *Archives of Applied Science Research*, 2011, 3 (3):154-166
24. Namasivayam C., Muniasamy N., Gayatri K., Rani M. & Ranganathan K., (1996), "Removal Of Dyes From Aqueous Solutions By Cellulosic Waste Orange Peel", *Bio resource Technology* 57 (1996) 37-43
25. Panda G.C., Das S.K. and Guha A.K., (2009) "Jute stick powder as a potential biomass for the removal of congo red and rhodamine B from their aqueous solution", *Journal of Hazardous Materials* 164 (2009) 374–379
26. Arivoli S And Thenkuzhali M., (2008), "Kinetic, Mechanistic, Thermodynamic & Equilibrium Studies on the Adsorption of basic dye Rhodamine B by Acid Activated Low Cost Carbon", *E-Journal of Chemistry*, Vol. 5, No.2, pp. 187-200, April 2008
27. Bhadusha N., and Anantha baskaran T., (2012), "Kinetic, Thermodynamic and Equilibrium Studies on Uptake of Rhodamine B onto ZnCl<sub>2</sub> Activated Low Cost Carbon", *E-Journal of Chemistry*, 2012, 9(1), 137-144
28. McCabe W.L, Smith J.C., Harriot P., Unit operations of chemical engineering, McGraw-Hill, Singapore (2005).
29. Ahmaruzzaman M., Gayatri S.L., (2011), "Activated Neem Leaf : A novel Adsorbent for the removal of Phenol, 4- Nitro phenols, and 4- chloro phenol from aqueous solution", *J. chem Eng. Data* 2011, 56, 3004-3016
30. Rengaraj S., Yeon K.H., Moon S.H., (2001), "Removal of chromium from waste and by ion exchange resins", *Journal of Hazardous Materials B87* (2001) 273-287
31. Kamal S., Ahmed F.E., Hussein F. G., Shokry G.E.B., Mamdoh R., (2011) " Removal of rhodamine B (a basic dye) and thoron (an acidic dye) from dilute aqueous solutions and wastewater simulants by ion flotation", 44 (2010) 1449-1461
32. Inbaraj B.S, Sulochana N., (2005) "Use of jackfruit peel carbon (JPC) for adsorption of rhodamine-B, a basic dye from aqueous solution", *Indian Journal of Chemical Technology*, Vol. 13, January 2006, 17-23
33. Uddin M.T., Islam M.S., Abedin M.Z., (2007), "Adsorption Of Phenol From Aqueous Solution By Water Hyacinth Ash", *Arpn Journal Of Engineering And Applied Sciences*, Volume : 2, Number:2, April 2007
34. C.E. Brewer, K. Schmidt-Rohr, J.A. Satrio, R.C. Brown, "Characterization of biochars from Fast Pyrolysis and Gasification systems", *Environmental Progress & Sustainable Energy* 28 (3) (2009) 386–396.



35. C.H. Cheng, J. Lehmann, "Ageing of black carbon along a temperature gradient", *Chemosphere* 75 (2009) 1021–1027.
36. Gode F., Pehlivan E., "Removal of Cr (III) from aqueous solution using lewatis S100: The effect of pH, time, metal concentration and temperature" ,*Journal of Hazardous Materials B* 136 (2006) 330-337
37. Khare P., Kumar A., "Removal of phenol from aqueous solution using carbonized Terminalia chebula-activated carbon: process parametric optimization using conventional method and Taguchi's experimental design, adsorption kinetic, equilibrium and thermodynamic study", *Appl. Water Sci.* (2012) 2:317–326
38. Al degs.Y.S.,Barghouthi M.I., El-sheikh A.H.,Walker G.M.," Effect of solution pH, ionic strength, and temperature on adsorption behaviour of reactive dyes on activated carbon", *Dyes and Pigments* 77 (2008) 16-23Chen .
39. S., Yue Q., Gao B., Xu X. , "Equilibrium and kinetic adsorption study of the adsorptive removal of Cr(VI) using modified wheat residue", *Journal of Colloid and Interface Science* 349 (2010) 256–264
40. Babic B.M., Milonjic S.K., Polovina M.J., Kaludierovic B.V., "Point of zero charge and intrinsic equilibrium constants of activated carbon cloth", *Carbon* 37 (1999) 477–481
41. Yorgun S., Vural N., Demiral H., "Preparation of high surface area activated carbons from paulownia wood by ZnCl<sub>2</sub> activation",*Microporous and mesoporous Materials* 122(2009)189-194
42. Yalcin N., evince V.,"Studies of the surface area and porosity of activated carbons prepared from rice husks", *carbon* 38 (2000) 1943-1945
43. Singh K, Risse M, Das K, Worley D, "determination of composition of cellulose and lignin mixtures using thermo gravimetric analysis (TGA)", 15th North American Waste to Energy Conference May 21-23, (2007), Miami, Florida USA